

Toward active x-ray telescopes II

Stephen L. O'Dell^{* a}, Thomas L. Aldroft^b, Carolyn Atkins^c, Timothy W. Button^d,
Vincenzo Cotroneo^b, William N. Davis^b, Peter Doel^e, Charlotte H. Feldman^f, Mark D. Freeman^b,
Mikhail V. Gubarev^a, Raegan L. Johnson-Wilke^g, Jeffery J. Kolodziejczak^a, Charles F. Lillie^h,
Alan G. Michetteⁱ, Brian D. Ramsey^a, Paul B. Reid^c, Daniel Rodriguez Sanmartin^j,
Timo T. Saha^k, Daniel A. Schwartz^b, Susan E. Trolrier-McKinstry^g, Melville P. Ulmer^l,
Rudeger H. T. Wilke^g, Richard Willingale^f, and William W. Zhang^k

^a NASA Marshall Space Flight Center, Astrophysics Office, Huntsville, AL 35812, USA

^b Harvard–Smithsonian Center for Astrophysics, 60 Garden St., Cambridge, MA 02138, USA

^c University of Alabama in Huntsville, Physics Department, Huntsville, AL 35899, USA

^d University of Birmingham, Metallurgy & Materials, Edgbaston, Birmingham B15 2TT, UK

^e University College London, Physics & Astronomy, Gower St., London WC1E 6BT, UK

^f University of Leicester, Physics & Astronomy, University Rd., Leicester, LE1 7RH, UK

^g Pennsylvania State University, Materials Research Institute, University Park, PA 16802, USA

^h Lillie Consulting, Playa del Rey, CA 90293, USA

ⁱ King's College London, Physics, The Strand, London, WC2R 2LS, UK

^j University of Brighton, Science & Engineering, Lewes Road, Brighton, BN2 4GJ, UK

^k NASA Goddard Space Flight Center, Greenbelt, MD 20771, USA

^l Northwestern University, Physics & Astronomy, Evanston, IL 60208-2900, USA

ABSTRACT

In the half century since the initial discovery of an astronomical (non-solar) x-ray source, the observation time required to achieve a given sensitivity has decreased by eight orders of magnitude. Largely responsible for this dramatic progress has been the refinement of the (grazing-incidence) focusing x-ray telescope, culminating with the exquisite sub-arcsecond imaging performance of the *Chandra X-ray Observatory*. The future of x-ray astronomy relies upon the development of x-ray telescopes with larger aperture areas ($> 1 \text{ m}^2$) and comparable or finer angular resolution ($< 1''$). Combined with the special requirements of grazing-incidence optics, the mass and envelope constraints of space-borne telescopes render such advances technologically challenging—requiring precision fabrication, alignment, and assembly of large areas ($> 200 \text{ m}^2$) of lightweight ($\approx 1 \text{ kg m}^{-2}$ areal density) mirrors. Achieving precise and stable alignment and figure control may entail active (in-space adjustable) x-ray optics. This paper discusses relevant programmatic and technological issues and summarizes current progress toward active x-ray telescopes.

Keywords: X-ray telescopes, x-ray optics, active optics, adjustable optics, bimorph actuators, piezoelectric devices, electrostrictive devices, magnetostrictive devices

1. INTRODUCTION

The *Chandra X-ray Observatory*^{1,2} (Figure 1) is the x-ray component of NASA's Great Observatories, a series of four in-space telescopes designed to probe cosmic sources over four electromagnetic bands—infrared (*Spitzer Space Telescope*), near-infrared-through-ultraviolet (*Hubble Space Telescope*), x-ray (*Chandra*), and γ -ray (*Compton Gamma-Ray Observatory*). Launched in 1999 and operating in a 63.5-hour high elliptical orbit, *Chandra* continues as a unique astrophysics facility for sub-arcsecond x-ray imaging.

* Contact author (SLO): stephen.l.odell@nasa.gov; voice +1 (256) 961-7776; fax +1 (256) 961-7522
Postal address: NASA/MSFC/ZP12; 320 Sparkman Drive NW; Huntsville, AL 35805-1912 USA



Figure 1. Illustration of NASA's *Chandra X-ray Observatory* in its operational configuration: 13.8-m length, 4.2-m diameter, 19.5-m wingspan, and 4800-kg (dry) mass. The *Chandra* flight system comprises the Telescope System (including the mirror assembly and optical bench—"tube"), the Spacecraft Module (surrounding the mirror assembly at one end of the optical bench), and the Integrated Science Instruments Module (containing two focal-plane detector arrays at the opposite end of the optical bench). [Credits: NGST]

With its sub-arcsecond mirror assembly and two focal-plane x-ray camera systems—the Advanced CCD for Imaging Spectroscopy³ (ACIS) and the High-Resolution Camera^{4,5} (HRC)—*Chandra* obtains exquisite x-ray images (Figure 2), at an angular resolution comparable to that of the best ground-based infrared–visible observatories. In addition, the sub-arcsecond mirror assembly enables high-resolution dispersive x-ray spectroscopy, upon insertion into the optical path of either of *Chandra*'s two objective transmission grating assemblies—the High-Energy Transmission Grating^{6,7} (HETG) and the Low-Energy Transmission Grating⁸ (LETG). While a few x-ray telescopes have somewhat larger aperture areas than does *Chandra*, none rivals its angular resolution. Indeed, the angular resolution of no past, present, or near-future astronomical x-ray telescope is within an order of magnitude as fine as that of *Chandra*. This fine resolution is essential for scientific investigations of the intricate structure of extended sources (Figure 2 left and center, as well as numerous other images at the *Chandra X-ray Center*'s web site⁹) and for the detection of faint point sources (Figure 2 right) against the charged-particle background or other cosmic sources.

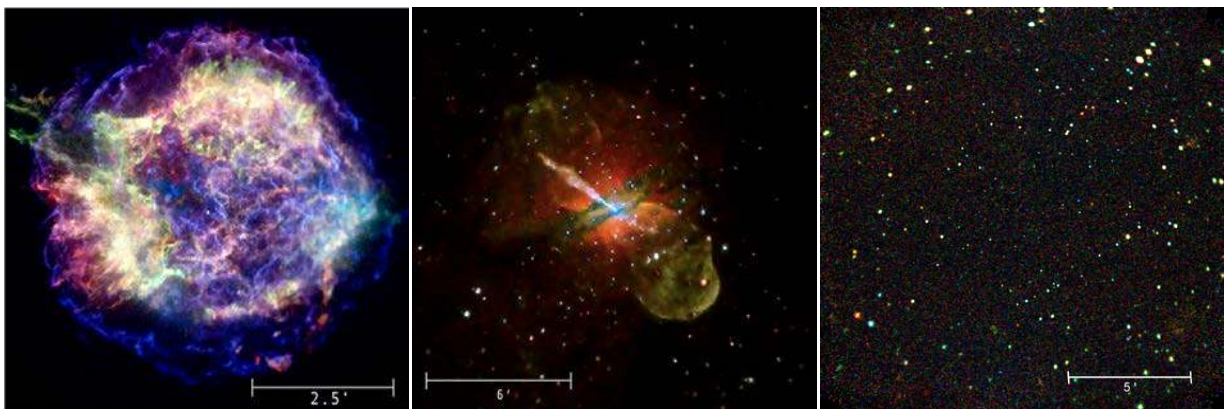


Figure 2. High-resolution x-ray color images obtained with the *Chandra X-ray Observatory*. The 300-year-old supernova remnant Cassiopeia A (left) exhibits diffuse thermal emission, synchrotron emission from shock-accelerated relativistic electrons, and a compact central object. The active galaxy Centaurus A (center) shows diffuse thermal emission with an absorption lane, a synchrotron-emitting jet and a faint counter jet each leading to a lobe over 10,000 light years from the active galactic nucleus (AGN), and many discrete stellar-mass x-ray sources within the galaxy as well as numerous background AGN. The *Chandra* Deep Field South (right) displays hundreds of AGN powered by supermassive black holes, as well as x-ray fainter galaxies, groups, and clusters of galaxies. [Credits: NASA/CXC/MIT/UMass/Stage et al. (left); NASA/CXC/CfA/Kraft et al. (center); NASA/JHU/AUI/Giacconi et al. (right)]

Future progress in high-energy astrophysics calls for an x-ray telescope with an aperture area at least an order of magnitude larger than *Chandra's* (0.11 m^2) and with comparable or finer angular resolution ($< 1''$). Here we first discuss considerations relevant to large-aperture-area ($> 1 \text{ m}^2$) sub-arcsecond x-ray telescopes (§2). Next we outline some potential paths for achieving this objective (§3), including utilization of active x-ray optics. Then we report on research to develop applicable actuator technologies (§4). Finally, we summarize the status of research toward active x-ray telescopes (§5).

2. CONSIDERATIONS

Development of large-aperture-area ($> 1 \text{ m}^2$) sub-arcsecond x-ray telescopes is a key objective to support further advances in high-energy astrophysics. Here we briefly address the motivation (§2.1) and discuss challenges (§2.2) in accomplishing this objective.

2.1. Motivation

For any astronomical telescope, the key performance metrics are angular resolution and aperture area. Finer angular resolution both improves imaging quality (Figure 3) and enhances sensitivity for detecting unresolved sources, by reducing the size of and thus number of background events in a telescope resolution pixel. Indeed, this reduction in background events is largely responsible for the 8-order-of-magnitude advantage of the *Chandra X-ray Observatory* over non-focusing (e.g., mechanical collimator or coded aperture) x-ray telescopes, in time to achieve a given background-limited detection. In fact, however, only the longest *Chandra* observations are close to background-limited for a point source. Indeed, the quiescent background rate in the 0.3-arcsec^2 *Chandra* (on-axis) resolution element is just a few times 10^{-7} s^{-1} !

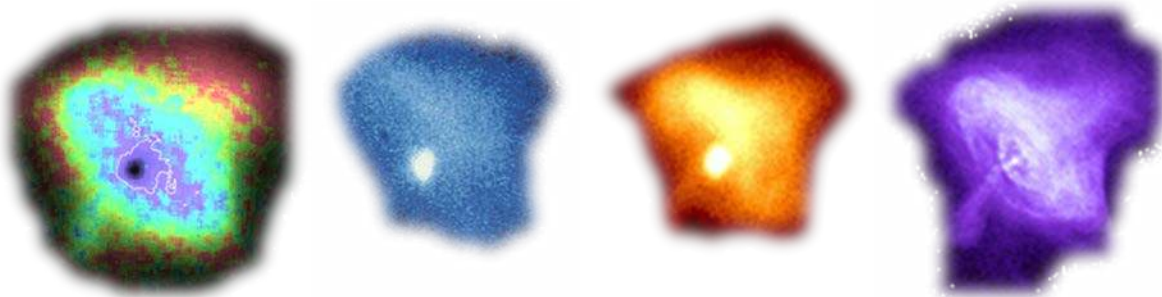


Figure 3. Comparison of x-ray images of the Crab Nebula obtained with high-resolution x-ray telescopes. From left to right, half-power-diameter (HPD) resolutions are approximately $15''$ (*XMM-Newton*, 1999–present), $10''$ (*Einstein Observatory*, 1978–1981), $5''$ (*Röntgen Satellit ROSAT*, 1990–1999), and $0.5''$ (*Chandra X-ray Observatory*, 1999–present). *Chandra's* sub-arcsecond resolution reveals the intricate structure of this pulsar wind nebula, powered by a rapidly rotating magnetized neutron star, the compact remnant of a supernova explosion in 1054.

Larger aperture area, of course, enhances sensitivity by increasing the signal. Furthermore, for extended sources, better angular resolution provides no improvement in signal-to-noise ratio once the source is resolved. However, collecting more photons becomes ineffective if adjacent sources are confused due to inadequate angular resolution. Thus, detection, identification, and study of fainter sources require both finer angular resolution and larger aperture area.

2.2. Challenges

As described briefly here, technical and programmatic considerations tend to make finer angular resolution and larger aperture area incompatible objectives. Obviously, using the same fabrication techniques to figure and to polish larger mirrors to the same or better precision is more costly and time-consuming. Furthermore, achieving larger aperture areas by reducing the areal mass typically decreases stiffness, hence increasing the propensity of the mirror to deform and thus to degrade imaging performance. While this applies to large ground-based telescopes, the constraints of in-space operation are even more demanding.

An additional challenge for x-ray telescopes is that, for the same *aperture area*, grazing-incidence mirrors require much more *surface area* than do normal-incidence mirrors. As grazing angles required for (near-total external) x-ray reflection are typically 1° (or less for higher-energy x rays), the surface-to-aperture ratio is of order 100 (or more). Consequently, if the same *areal mass* and fabrication techniques were used, the mass, cost, and schedule would each be roughly a couple hundred times (or more for hard x rays) larger for an x-ray (grazing-incidence) telescope than for a normal-incidence telescope of the same *aperture area*.

To appreciate better the technical and programmatic challenges in producing a large-area ($> 1 \text{ m}^2$ aperture) sub-arcsecond x-ray telescope, we review the characteristics of *Chandra's* sub-arcsecond High-Resolution Mirror Assembly (HRMA). Figure 4 shows a schematic (left) and during-assembly photograph (right) of the HRMA. Danbury Optical Systems (then owned by Hughes) precision figured and superpolished the 8 mirror shells (4 mirror pairs) from Zerodur™ thick-walled ($\approx 2\text{-cm}$ thick) conic frusta, using conventional mechanical lapping and polishing combined with precision metrology. Eastman Kodak designed the HRMA structure and precision aligned and mounted the mirror shells into the HRMA. This approach was remarkably successful for *Chandra*, achieving its sub-arcsecond resolution. However, scaling this approach to larger x-ray telescopes would confront several issues, the major ones being mass (§2.2.1), envelope (§2.2.2), and cost (§2.2.3).

2.2.1. Mass

Due to the thick walls needed to ensure sufficient stiffness during mechanical processing of the precision mirror surfaces, *Chandra's* Zerodur™ (2.53 specific density) mirrors have an areal density of about 50 kg m^{-2} . Due to the grazing-angle projection factor plus the fact that each secondary mirror is roughly the same size as its corresponding primary, obtaining *Chandra's* 0.11 m^2 *aperture area* requires nearly 20 m^2 precision optical *surface area*. Thus the total mass of the mirrors alone is about 1 tonne. Adding structure and collimators to its mirrors, the HRMA mass is about 1.5 tonne—nearly one-third the dry mass of the entire *Chandra* observatory (Figure 1).

Mass constraints on in-space operation render it infeasible simply to build a *Chandra*-like x-ray telescope with an aperture area that is larger by an order of magnitude. Thus achieving a large aperture area ($> 1 \text{ m}^2$) requires lightweight (areal density $\approx 1 \text{ kg m}^{-2} < 5 \text{ kg m}^{-2}$) grazing-incidence mirrors. The technical challenge is, of course, to construct a precision sub-arcsecond x-ray telescope using such lightweight mirrors.

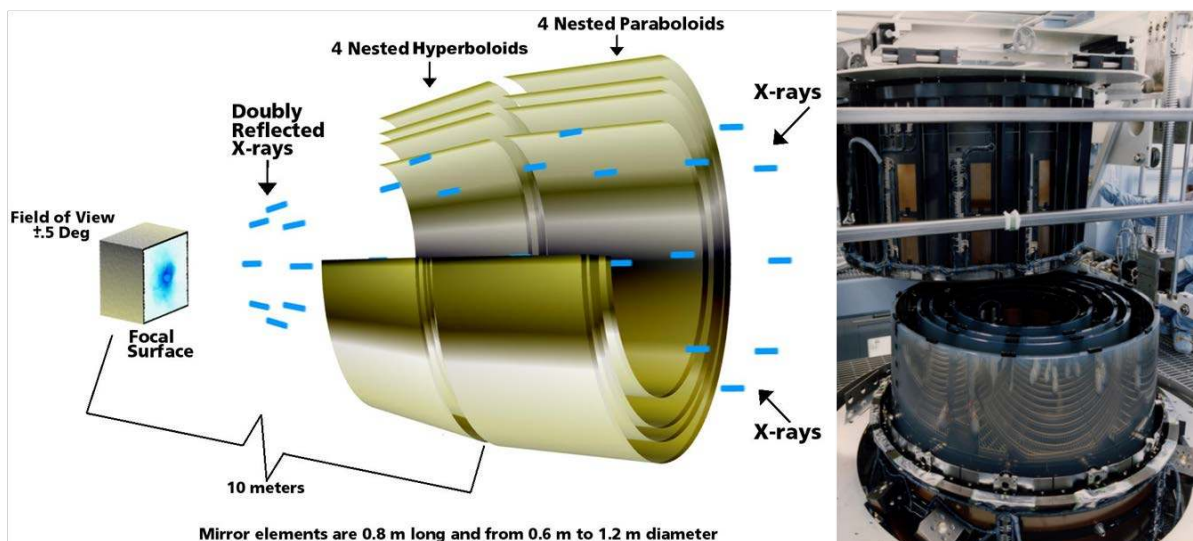


Figure 4. Schematic of the mirror configuration (left) for the *Chandra* High-Resolution Mirror Assembly (HRMA), shown (right) during alignment and assembly. The HRMA contains 4 co-aligned Wolter-1 (paraboloid–hyperboloid) grazing-incidence mirror pairs, with a 10-m focal length. Each of the 8 full-shell Zerodur™ mirrors is 84-cm long, with (intersection-plane) diameters 63–120 cm and thicknesses 1.6–2.4 cm. [Credits: NASA/CXC/Berry (left); Kodak (right)]

2.2.2. Envelope

Envelope constraints on in-space operation also render it impractical to build an order-of-magnitude larger *Chandra*-like x-ray telescope. A 10-times larger aperture area would require multiplying the diameter and focal length by about 3 ($\approx \sqrt[3]{10}$), in order to achieve the grazing-angle range and energy response. Besides necessitating an extensible optical bench to reach a 30-m focal length, the larger-diameter mirrors would need to be proportionately thicker to preserve their relative stiffness. This would lead to a factor-of-30 mass growth, further compounding the already untenable mass issue (§2.2.1). The most efficient way to increase the aperture area, without unrealistically pushing the envelope constraints, is to increase the packing density of the nested grazing-incidence mirror pairs—i.e., to increase the fraction of the available transverse envelope (maximum aperture) that is open.

The open-aperture fraction of *Chandra*'s HRMA is only about 15%, partly because it is loosely packed due to elimination of 2 of the original 6 mirror pairs in re-scoping the mission from a near-earth Shuttle-serviced orbit to a high elliptical orbit. (Thus, the HRMA mirror pairs are still numbered 1, 3, 4, and 6.) However, even if the mirror pairs were optimally packed, the thickness of the mirrors would limit the open-aperture fraction to about 30%. Thus, mirror thickness is an envelope issue as well as a mass issue. Using lower-density substrates of approximately the same thickness as the *Chandra* mirrors would reduce mass but not increase the open-aperture fraction. Substantially increasing the open-aperture fraction calls for thin (≤ 1 mm, depending upon length) grazing-incidence mirrors.

2.2.3. Cost

The cost of the *Chandra* HRMA was very roughly 0.6 G\$ in 2012 US dollars, including both non-recurrent (facilities, equipment, design, process development, etc.) and recurrent (per-unit incremental) costs. Amortizing all HRMA costs over the 4 flight mirror pairs (20 m² surface area) gives a price of about 30 M\$ m⁻² of precision mirror surface. More difficult to calculate is the incremental cost of fabricating additional mirrors of the comparable quality, using similar fabrication methods. However, a reasonable estimate would seem to be in the range 10–20 M\$ of precision mirror surface. This is somewhat higher than the 5–10 M\$ m⁻² typical estimate for large, monolithic normal-incidence mirrors used in ground-based observatories.

Based upon these considerations, the estimated cost to build a *Chandra*-like mirror assembly with 10 times the area, using *Chandra*-like fabrication methods, would be 2–4 G\$ for about 200 m² precision optical surface area. This would drive the total mission cost to roughly 5 G\$ or so, which seems untenable in the current economic environment.

Precision fabricating mirrors with 10 times the surface area of the *Chandra* mirrors within a *Chandra*-scale budget would require a proportionate decrease in the areal cost of the mirrors and mirror assembly—i.e., areal cost ≈ 1 M\$ m⁻² < 3 M\$ m⁻². Such a reduction would in turn require either a significant decrease in the cost of direct fabrication of precision mirrors or the use of replicated optics. In the latter case, the cost of precision fabrication of each mandrel (presumably comparable to the cost of direct fabrication of a mirror of comparable area) is amortized over several-to-many mirrors replicated from each mandrel. The current state of the art for replicated x-ray optics—the electroformed-nickel shells of the XMM-*Newton* mission or the slumped-glass segmented mirrors under technology development—achieves half-power diameters HPD $\approx 15''$, 30 times coarser than *Chandra*'s angular resolution.

The cost savings inherent in replication obviously depends upon multiplicity. Employing a large number of identical mirrors in an x-ray telescope forces modularity and favors segmented (rather than full-shell) designs. An array of full-shell modules—i.e., smaller, complete mirror assemblies—is advantageous in terms of the optics and has been used in XMM-*Newton* and other (smaller) x-ray observatories. However, as this approach requires a separate focal-plane detector for each mirror assembly, it is feasible only if resource (mass, power, cost) demands of each detector are small.

3. POTENTIAL PATHS

The *Chandra* approach to producing sub-arcsecond x-ray optics was exceptionally successful. However, as discussed (§2.2), this approach is not scalable to the larger collecting areas required for a future facility-class x-ray observatory.

1. Mass constraints (§2.2.1) require lightweight mirrors, with areal density ≈ 1 kg m⁻² < 5 kg m⁻².
2. Envelope constraints (§2.2.2) require thinner mirrors, with thickness ≤ 1 mm (depending upon mirror length).
3. Cost constraints (§2.2.3) demand less expensive mirror fabrication, with an areal cost ≈ 1 M\$ m⁻² < 3 M\$ m⁻².

To be concise, achieving an order-of-magnitude larger collecting area will require roughly an order-of-magnitude reduction in areal density, thickness, and areal cost of the x-ray mirrors. Evolving toward even larger collecting areas will necessitate further reductions in magnitude of these three parameters. How then might one construct a sub-arcsecond x-ray telescope using lightweight, thin, (relatively) inexpensive mirrors? Recall that the bending stiffness of a simple beam is proportional to $E w (h/l)^3$, with E the material's elastic modulus, w the width, h the thickness, and l its length or span. Thus, the stiffness is a sensitive function of the thickness-to-span ratio (h/l).

As mounting-induced and gravity-induced distortions of thin mirror are potentially severe at long spatial wavelengths, the mounting and assembly scheme needs to be able to correct low-spatial-frequency deviations. As mounting is unlikely to correct figure errors at mid and short spatial wavelengths, one needs to start with mirrors that are inherently sub-arcsecond quality at least at mid and higher spatial frequencies. For this discussion, we assume that mirrors of such quality can be produced and focus on schemes to mount the mirrors into an assembly.

Here we outline two general paths for controlling or correcting mirror distortion induced by mounting stresses or gravity. The first path—followed for every high-resolution (HPD < 10") x-ray telescope to date—is to utilize rigid (stiff) optics (§3.1), which are minimally susceptible to distortion. The second path—employed for most modern large normal-incidence telescopes and for some x-ray mirrors at synchrotron light sources—is to implement active (adjustable) optics (§3.2), which are actively deformed to compensate for low-order figure errors.

3.1. Rigid optics

All x-ray telescopes with angular resolution finer than 10" have used full-shell thick-walled mirrors for stiffness during fabrication, metrology, alignment and mounting, and operation. Unfortunately, this technology cannot satisfy the mass, envelope, and cost constraints to provide the large aperture areas needed for future facility-class x-ray telescopes. As mentioned previously, thick mirrors of low-density materials might address the mass issue (§2.2.1) but does not solve the envelope problem (§2.2.2) that thick walls result in low open-aperture fractions.

A viable approach for achieving high stiffness using thin-walled mirrors is to fabricate the mirror module as an integral structure. Figure 5 left panel displays a prototype silicon-pore optic^{10,11,12} (SPO) fabricated (largely robotically¹³) by cosine BV for ESA's European Space Research & Technology Centre (ESTEC). The mirror module contains dozens of diced, ribbed, and wedged silicon plates, which are robotically stacked into the X-ray Optics Unit (XOU). If ESA is able to fabricate XOUs meeting the angular-resolution goal (HPD < 5"), such a stiff structure would ensure preservation of the angular resolution. Of course, achieving sub-arcsecond resolution with such an approach will be much more difficult. That each mirror is severely over-constrained ensures stiffness; but it also means that the constraints are likely to deform the mirror from its free figure. However, precision control of the constraints—e.g., by precision figuring of the silicon-wafer rib edges—could impart the desired shape on the mirror.

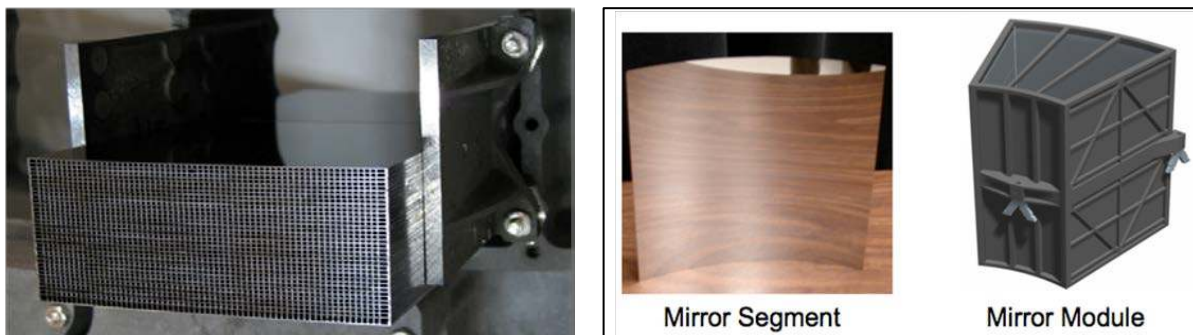


Figure 5. Contrasting approaches to mounting lightweight ($\approx 1 \text{ kg/m}^2$) grazing-incidence mirrors for segmented x-ray telescopes. Silicon pore optics (left), being developed by ESA, utilize integrated structure to produce a highly over-constrained mount that provides exceptional stiffness. Slumped-glass optics (right), being developed by NASA, employ discrete mounting points along the mirror edges to align and to hold minimally over-constrained mirrors within a mirror module. [ESA/cosine/MPE/KT/SRON/Micronit/Bavdaz (left); NASA/GSFC/Zhang (right)]

In contrast with ESA's XO (Figure 5 left), NASA's mirror module (Figure 5 right) for a large x-ray mirror assembly would mount thin (0.4 mm) slumped-glass mirrors^{14,15,16} (Figure 5 right) using only a few attachment points along the mirror edges. Such a mounting scheme minimally constrains the mirrors—either to preserve the free shape of the mirror or to provide minor long-wavelength figure correction during alignment and bonding.

Technology development of silicon pore optics and of slumped-glass optics for x-ray telescopes has thus far demonstrated imaging performance at the module or smaller level of HPD $\approx 15''$. This is comparable to the system-level imaging performance of XMM-Newton, but with a mirror areal density about an order of magnitude less— 1 kg m^{-2} versus 10 kg m^{-2} for XMM-Newton and 50 kg m^{-2} for Chandra. The objective of either of these technology programs is to enable a system-level HPD of $10''$ with a goal of $5''$ —i.e., a resolution as much as 3 times finer than that of XMM-Newton but still 10 times coarser than that of Chandra.

While each of these approaches to lightweight x-ray telescopes address the issues of mass, envelope, and cost in scaling up the collecting areas for x-ray observatories, neither is likely to achieve an angular resolution close to that of Chandra. Doing so will require much better control or correction of mount-induced and gravity-induced figure errors—either through integral structure to increase stiffness, radically improved mounting techniques to minimize distortion, or *in situ* figure correction. Regarding *in situ* figure correction, there are two general approaches. One is *in situ* surface processing of the mirrors—by low-force removal or addition (e.g., differential deposition) of mirror material to correct residual figure errors after mounting, but without increasing surface roughness. Another is *in situ* adjustment of the mounted mirrors using active optics techniques (§3.2).

3.2. Active optics

Modern, large normal-incidence telescopes employ active optics to orient mirrors or to correct figure at low-to-mid spatial frequencies. At intermediate cadence, these adjustments correct for distortions due to gravity, temperature changes, etc. At rapid cadence, they correct wavefront fluctuations due to atmospheric turbulence. Synchrotron light sources now use active grazing-incidence optics (at relatively slow cadence) to adjust curvature and low-order figure of small x-ray mirrors. Within the past decade, x-ray astronomers began investigating active optics with the goal of achieving sub-arcsecond resolution for large, lightweight x-ray telescopes. In the UK, the Smart X-ray Optics consortium^{17,18,19} (2005–2010) implemented the first comprehensive research program. In the US, two mission concepts—Generation-X^{20,21,22,23,24} and SMART-X²⁵ (Figure 6)—have motivated technology development for active x-ray telescopes.

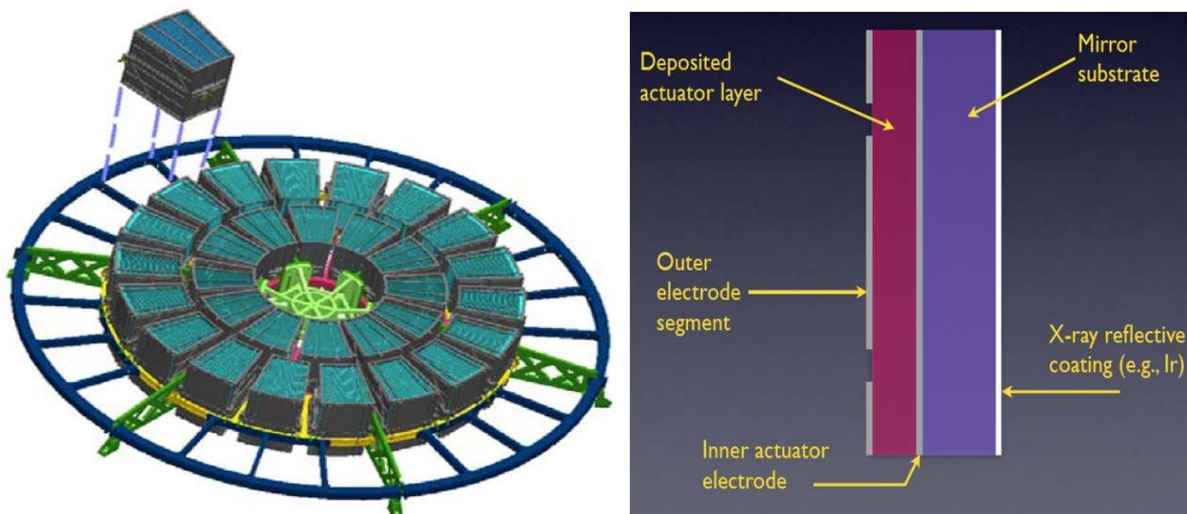


Figure 6. Concept for a large-aperture-area ($> 1 \text{ m}^2$) fine-resolution ($< 1''$) x-ray telescope (SMART-X), which would achieve the angular resolution of Chandra but with an order-of-magnitude more area. The mirror assembly (left) would leverage technologies developed for the *International X-ray Observatory* and similar proposed missions, but incorporate piston and electro-active bimorph actuators (right) to adjust alignment and to correct surface figure. [Credits: SAO/PSU/Schwartz et al.]

The active-optics approach toward developing a sub-arcsecond x-ray telescope is multifaceted. It leverages off existing x-ray technology development to start with good (HPD $\approx 5''$) lightweight mirrors, such as the slumped-glass mirrors (§3.1 and Figure 5 right) being developed for NASA’s next facility-class x-ray telescope. Indeed, the SMART-X mission concept (Figure 6 left) is very similar, differing fundamentally only in the incorporation of active x-ray optics (Figure 6 right). Such mirrors have mid- and high-frequency surface errors that are sufficiently small to allow imaging resolution at about 1'' HPD if the low-frequency figure errors can be corrected. Of course, it is important to minimize low-frequency errors—whether due to manufacturing deviations or to mount-induced distortions—as much as feasible before applying active-optics techniques to adjust alignment and to correct mirror figure at low-to-mid spatial frequencies.

Research is underway to develop, analyze, measure, characterize, and test actuator technologies (§4) for individual mirrors suited for the special geometry of highly nested, lightweight, grazing-incidence optics. Besides addressing the actuator technologies for individual mirrors, it is essential to formulate strategies for diagnosing and correcting alignment and figure errors for the large number of mirrors required to build a large-aperture-area x-ray telescope comprised of numerous mirror modules, each containing of-order-hundred highly nested segmented mirrors. To implement this strategy for on-ground characterization and in-space operation will require sophisticated control algorithms and auxiliary hardware. As the diagnostic and adjustment scheme is likely to be complicated and time consuming, it is important that in-space adjustment be infrequent. This in turn will likely require tight thermal control of the mirror assembly, as well as excellent repeatability and stability of the actuators themselves.

4. ACTUATOR TECHNOLOGIES

Here we briefly describe the various actuator technologies under development for active x-ray telescopes. More detailed descriptions are in this Volume and elsewhere.

There are fundamentally two categories of actuation, based upon how force is applied to the mirror. *Surface-normal actuation* (SNA, §4.1) acts as a piston to move the mirror for rigid-body alignment, or to effect a global or local deformation of the mirror. *Surface-tangential actuation* (STA, §4.2) acts as a bimorph in combination with the mirror substrate to effect local deformation of the mirror.

4.1. Surface-normal actuators (pistons)

SNA has limited applicability to x-ray telescopes as it requires a reaction structure, which is largely incompatible with the mass and envelope constraints on a highly nested grazing-incidence mirror assembly. Nonetheless, SNA is suited for adjusting alignment and for correcting some low-frequency errors (Figure 7).

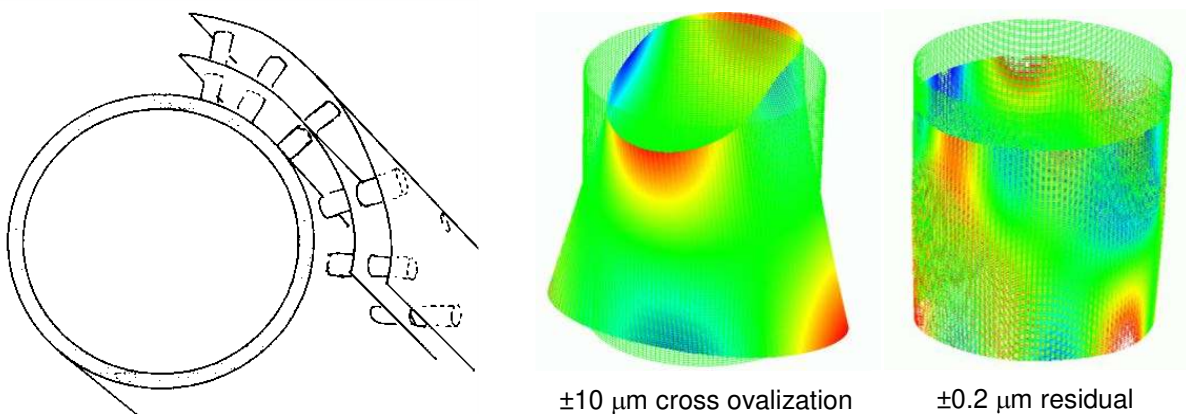


Figure 7. Discrete (piston) surface-normal actuators (SNA) for alignment and low-order figure correction of lightweight ($\approx 1 \text{ kg/m}^2$) full-shell grazing-incidence mirrors. A thick-walled conic frustum (left) serves as a reaction structure for discrete piston actuators acting radially upon successive nested shells. Finite element analysis (FEA) indicates that this approach can correct distortion modes such as cross ovalization (center) to very good precision (right). The FEA here assumes 8×10 pistons acting on a single shell, with no non-radial linkage. [Credits: SAO/Reid et al.]

The Smithsonian Astrophysical Observatory (SAO) is leading an effort to improve the imaging performance of thin, full-shell mirrors from current values of HPD $\approx 15''$ – $20''$ to a goal of $5''$, through the use of discrete electro-active (SNA) pistons mounted in a coarse array (Figure 7 left) and reacting against a stiff (thick-walled) inner frustum. The research program utilizes thin-walled (≈ 0.2 mm) electroformed-nickel replicated full-shell mirrors from NASA Marshall Space Flight Center and electrostrictive—unpoled lead magnesium niobate (PMN) ceramic—piston actuators produced by Northrop-Grumman AOA-Xinetics.

Finite-element analysis indicates that this approach can in principle correct certain low-order figure distortions (Figure 7 center) to reasonably good accuracy (Figure 7 right). As the research program started just recently, there are as yet no results to report. While this approach might achieve the $5''$ goal, reaching sub-arcsecond performance likely requires other approaches.

4.2. Surface-tangential actuators (bimorphs)

As just discussed (§4.1), SNA (piston) actuation may be useful in positioning mirror modules or individual mirrors or even correcting some low-order figure errors. However, owing to mass and envelope constraints, applying active-optics techniques to the special geometry of nested grazing-incidence mirrors, calls for use of STA (bimorph) actuation to correct low-to-mid frequency surface errors. Here we briefly describe four research efforts to develop STA technologies for high-resolution x-ray telescopes. More detailed descriptions appear in other articles in this Volume.

4.2.1. Bonded electro-active pads

The Smart X-ray Optics (SXO) consortium (2005–2010) undertook a comprehensive end-to-end research program in the UK to develop and demonstrate active x-ray optics for astronomical applications²⁶. In particular, the University of Birmingham led fabrication of piezoelectric—poled lead zirconate titanate (PZT) ceramic—shaped pads²⁷ (Figure 8 left) using viscous plastic processing (VPP). University College London (UCL) led mandrel fabrication and replication of thin (0.4 mm) electroformed-nickel mirror segments^{28,29} (Figure 8 center), to which the shaped PZT pads were bonded. UCL and STFC Daresbury Laboratory conducted finite-element analysis³⁰ (FEA) and performed metrology. Meanwhile the University of Leicester carried out performance predictions³¹ and x-ray testing³² (Figure 8 right).

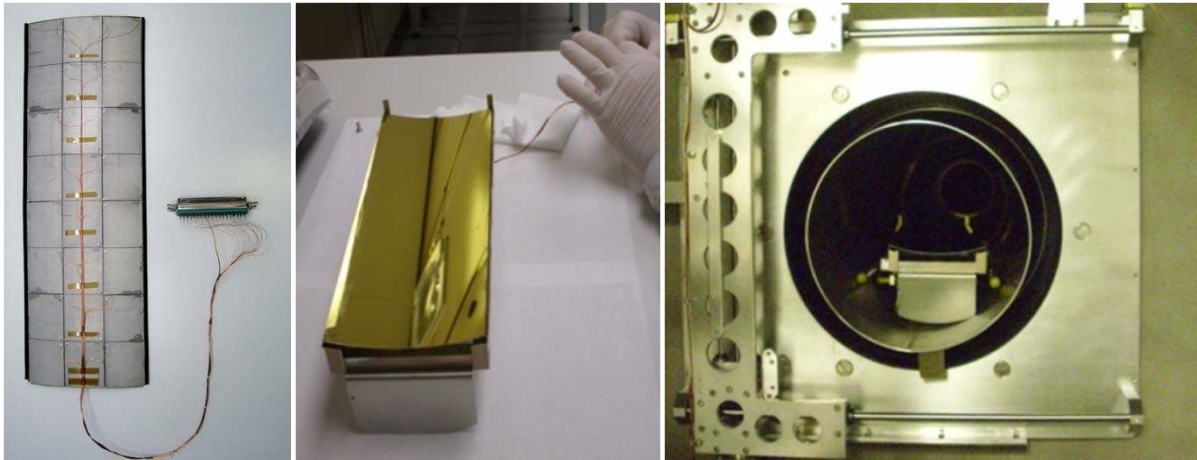


Figure 8. Electro-active surface-tangential actuators (STA) bonded to the back of a lightweight (≈ 1 kg/m²) segmented grazing-incidence mirror. Electrical leads to individual pads (left) allow controlled STA bimorph deformation to address low-order figure errors in the mirror (center). Metrology and x-ray testing (right) assess the efficacy of the correction. [Credits: UBirmingham/UCLondon/ULeicester/Feldman et al.]

This pioneering effort was impressive for its scope and showed that such an approach can deform thin mirrors. However, the measured imaging performance was of order an arcminute, due to inherent mirror figure errors and to print-through from the glued PZT pads.

4.2.2. Bonded electro-active lattice

Northrop-Grumman AOA-Xinetics has developed both surface-normal and surface-tangential electrostrictive—unpoled lead magnesium niobate (PMN) ceramic—actuators for active optics. Since 2008, AOA-Xinetics has been developing active optics for x-ray applications³³—including x-ray telescopes and synchrotron light sources. Most relevant for correction of low-to-mid-frequency deviations of mirror surfaces in large-area x-ray telescopes are the PMN lattices (Figure 9 left) with individually addressable nodes (Figure 9 center). Activation of a lattice node effects surface-tangential actuation (STA) to locally deform the mirror onto which the lattice is bonded (Figure 9 right).

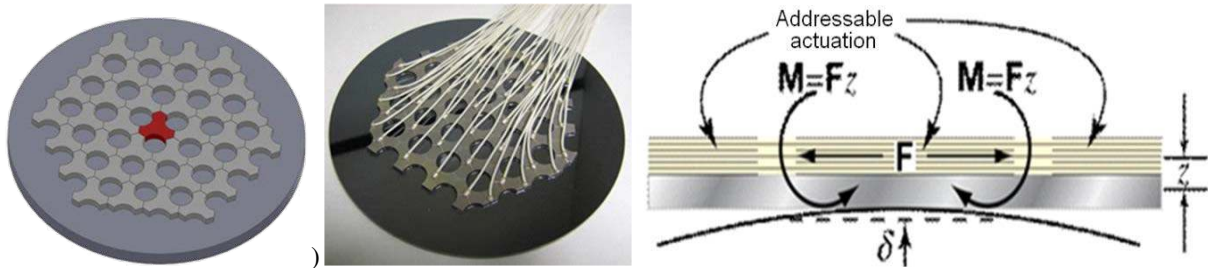


Figure 9. Lattice of individually addressable electro-active surface-tangential actuators (STA) bonded to the back of a lightweight ($\approx 1 \text{ kg/m}^2$) segmented grazing-incidence mirror. Each electro-active trefoil node (left) is electrically isolated and individually activated by voltage applied to the node (center). The consequent local STA bimorph deformation (right) addresses figure errors on scales as small as twice the lattice spacing. [Credits: NG AOA-Xinetics/Lillie et al.]

4.2.3. Thin-film electro-active array

Motivated initially by the Generation-X mission concept and more recently by the SMART-X mission concept, the Smithsonian Astrophysical Observatory (SAO) is leading a comprehensive research program to develop, model, characterize, and test technologies for active x-ray telescopes. Development of actuator technology is emphasizing arrays of thin-film piezoelectric—poled lead zirconate titanate (PZT) ceramic—actuators. Pennsylvania State University (PSU) is developing this thin-film actuator technology^{34,35}, which sputters (Figure 10 left) a uniform ground-electrode layer, a uniform PZT layer, and then a patterned electrode layer with conductive traces onto the back of a segmented mirror (Figure 10 right).

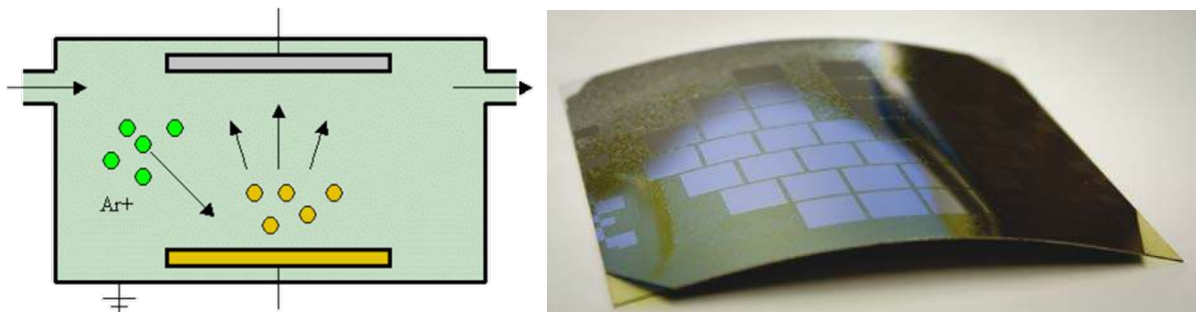


Figure 10. Patterned array of individually addressable electro-active surface-tangential actuators (STA), electrodes, and traces deposited (left) onto the back of a lightweight ($\approx 1 \text{ kg/m}^2$) slumped-glass grazing-incidence mirror (right). Through bimorph deformation, each electro-active pixel addresses figure errors on scales as small as twice the pixel spacing. [Credits: SAO/PSU/Johnson-Wilke et al.]

Perhaps the most troublesome feature of this approach for slumped-glass mirrors (Figure 10 right) is that the PZT must be crystallized and annealed at a relatively high temperature ($\approx 550^\circ$), which is close to the softening temperature of many glass formulations. The identification of a glass—a Corning Eagle formulation—with a somewhat higher softening temperature has somewhat mitigated this problem³⁶. PSU has successfully produced partially functioning thin-film piezoelectric arrays on optical flats of this glass formulation (Figure 11 left), which are used during process development and measured (Figure 11 right) for influence-function characterization³⁷ (Figure 12).

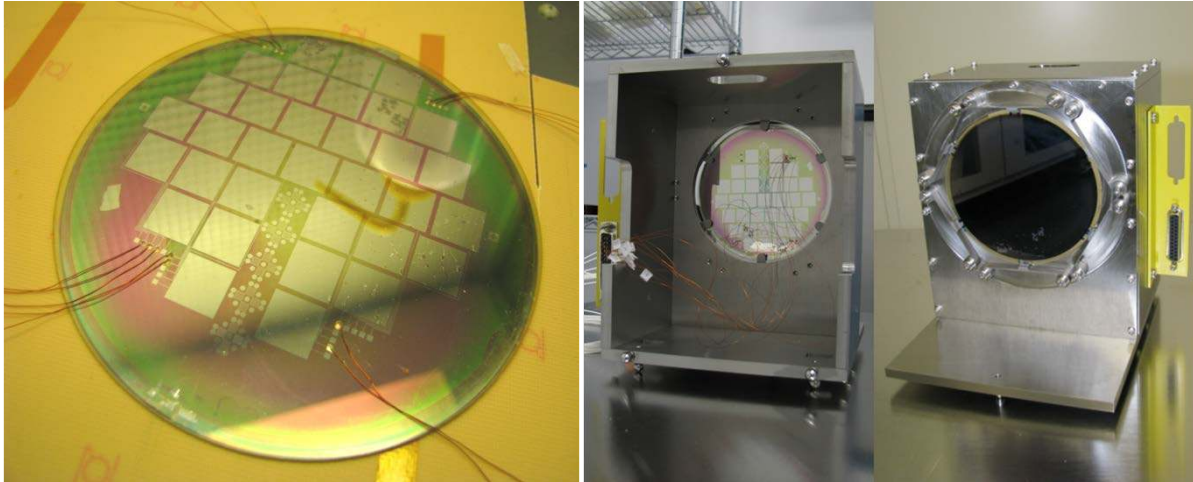


Figure 11. Measurement of the influence function for a patterned array of electro-active surface-tangential actuators (STA). A 100-mm-diameter optical flat with the patterned array deposited onto its back (left) is mounted into a holding fixture (right) for a sequence of metrology measurements of the optical surface for various actuation settings. [Credits: SAO/PSU/Cotroneo et al.]

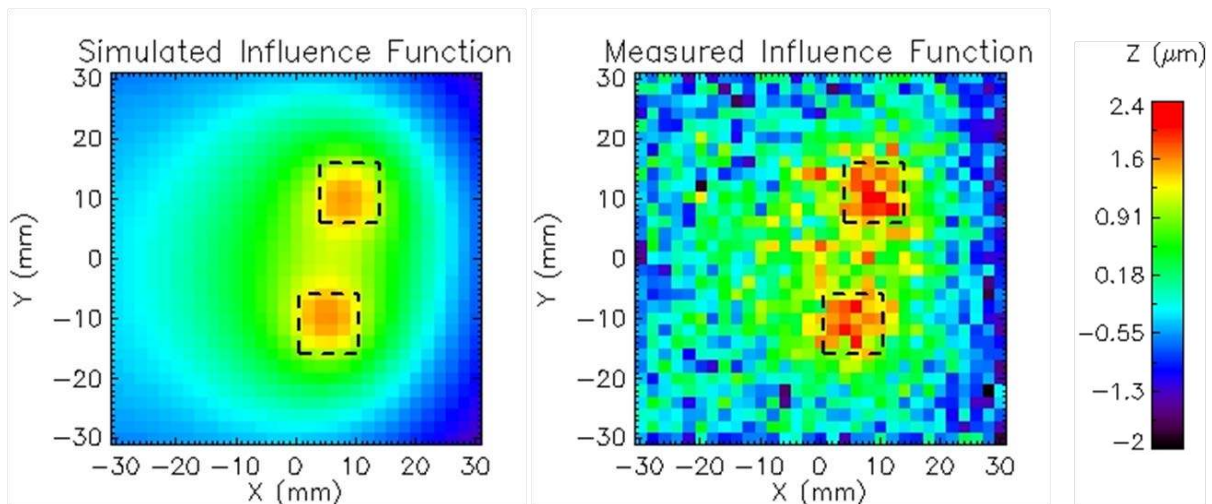


Figure 12. Comparison of the influence function for activation of two 10-mm-square electro-active STA pixels, as simulated (left) using finite-element analysis and as measured (right) on a coordinate measuring machine. [Credits: SAO/PSU/Cotroneo et al.]

4.2.4. Magnetic writing

Magneto-active materials are a novel alternative to electro-active materials for effecting surface-tangential actuation (STA) to effect bimorph deformation of a mirror^{38,39}. This approach envisions using magnetic smart materials to enable the writing of figure corrections into a mirror, analogous to a magnetic head writing data onto a hard drive. Figure 13 left illustrates the concept: An applied magnetic field produces STA in a highly magnetostrictive layer; the applied magnetic field also magnetizes a magnetically hard under-layer or substrate that retains the magnetic field even after the writing magnet is removed; bimorph deformation persists as long as the under-layer or substrate remains magnetized.

Northwestern University is pursuing a comprehensive program to demonstrate proof of concept⁴⁰. The Northwestern team electroforms nickel mirrors that serve as the high-coercivity ferromagnetic substrate, sputters a magnetostrictive material onto the back of the mirror, measures the magneto-active deformation using a white-light interferometer in tandem with the magnetic writing head (Figure 13 right), and compares experimental results with FEA predictions⁴¹.

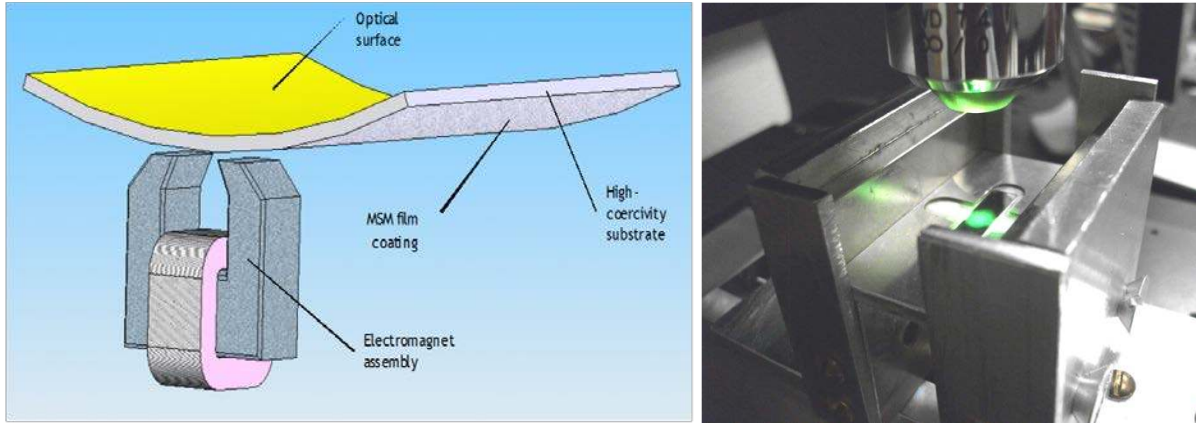


Figure 13. Magnetic writing of corrections to the figure of a grazing-incidence mirror. The schematic (left) illustrates this proposed approach, in which an applied magnetic field produces surface-tangential actuation in a magnetostrictive coating over a high-coercivity magnetic substrate. Changing the applied magnetic field as the “write head” moves over the mirror effects non-uniform bimorph deformation of the substrate, which would correct the intrinsic surface figure errors. A white-light interferometer aligned with the magnetic head (right) measures the applied bimorph deformation.

5. SUMMARY

Creating a large-aperture-area ($> 1 \text{ m}^2$) sub-arcsecond x-ray telescope will be technologically and programmatically challenging. Achieving sub-arcsecond imaging with the thin, lightweight ($\approx 1 \text{ kg m}^{-2} < 5 \text{ kg m}^{-2}$) mirrors needed to satisfy mass and envelope constraints requires significant advancement of technologies. Further, to be programmatically viable, areal costs for mirror fabrication and alignment and assembly must be relatively low ($< 1 \text{ M\$ m}^{-2} < 3 \text{ M\$ m}^{-2}$).

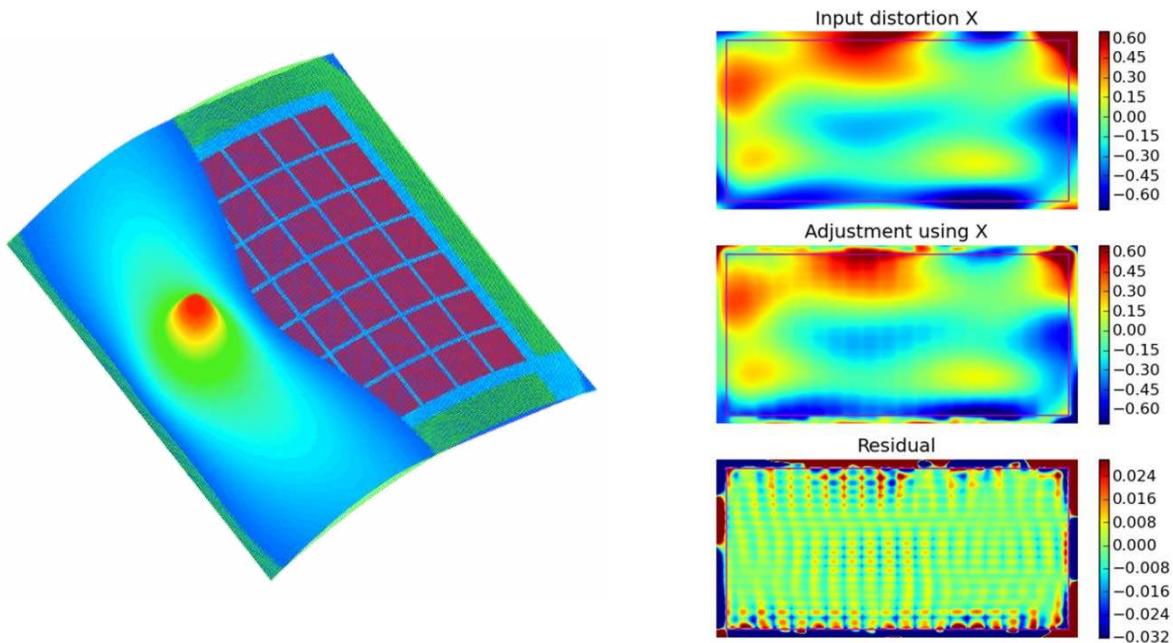


Figure 14. Computational assessment of efficacy of an electro-active array in correcting arbitrary surface figure errors. Using influence functions from FEA simulations (left), an assumed initial distortion (right top) is corrected using an optimal adjustment (right middle), leaving a residual distortion (right bottom). [Credits: SAO/Aldcroft et al.]

Achieving precise and stable alignment and figure control may entail active (in-space adjustable) x-ray optics. Research is underway to develop actuator technologies consistent with the special geometry of densely packed grazing incidence mirrors. For alignment and correction of some low-order figure errors, surface-normal actuation (SNA)—piston-like deformation, as traditionally used for active normal-incidence mirrors—is appropriate. However, for correction of low-to-mid-order figure errors, surface-tangential actuation (STA)—bimorph deformation—is needed.

Here we briefly described research programs to develop actuator technologies particularly suited to x-ray telescopes. While research in active x-ray telescopes has progressed notably over the past few years, the field is still in its infancy. Nonetheless, the potential to correct actively the figure of mounted grazing-incidence mirrors (Figure 14⁴²) is exciting.

REFERENCES

-
- ¹ O'Dell, S. L., & Weisskopf, M. C., "The role of project science in the Chandra X-ray Observatory", SPIE 6271, 07:1-14 (2006).
 - ² Weisskopf, M. C., Tananbaum, H. D., Van Speybroeck, L. P., & O'Dell, S. L., "Chandra X-ray Observatory (CXO): overview", SPIE 4012, 2-16 (2000).
 - ³ Garmire, G. P., Bautz, M. W., Ford, P. G., Nousek, J. A., & Ricker, G. R., Jr., "Advanced CCD imaging spectrometer (ACIS) instrument on the Chandra X-ray Observatory", SPIE 4851, 28-44 (2003).
 - ⁴ Kenter, A. T., Chappell, J. H., Kraft, R. P., Meehan, G. R., Murray, S. S., Zombeck, M. V., Hole, K. T., Juda, M., Donnelly, R. H., Patnaude, D., Pease, D. O., Wilton, C., Zhao, P., Austin, G. K., Fraser, G. W., Pearson, J. F., Lees, J. E., Brunton, A. N., Barbera, M., Collura, A., & Serio, S., "In-flight performance and calibration of the Chandra high-resolution camera imager (HRC-I)", SPIE 4012, 467-492 (2000).
 - ⁵ Kraft, R. P., Chappell, J. H., Kenter, A. T., Meehan, G. R., Murray, S. S., Zombeck, M. V., Donnelly, R. H., Drake, J. J., Johnson, C. O., Juda, M., Patnaude, D., Pease, D. O., Ratzlaff, P. W., Wargelin, B. J., Zhao, P., Austin, G. K., Fraser, G. W., Pearson, J. F., Lees, J. E., Brunton, A. N., Barbera, M., Collura, A., & Serio, S., "In-flight performance and calibration of the Chandra high-resolution camera spectroscopic readout (HRC-S)", SPIE 4012, 493-517 (2000).
 - ⁶ Markert, T. H., Canizares, C. R., Dewey, D., McGuirk, M., Pak, C. S., & Schattenburg, M. L., "High-Energy Transmission Grating Spectrometer for the Advanced X-ray Astrophysics Facility (AXAF)", SPIE 2280, 168-180 (1994).
 - ⁷ Canizares, C. R., Davis, J. E., Dewey, D., Flanagan, K. A., Galton, E. B., Huenemoerder, D. P., Ishibashi, K., Markert, T. H., Marshall, H. L., McGuirk, M., Schattenburg, M. L., Schulz, N. S., Smith, H. I., & Wise, M., "The Chandra High-Energy Transmission Grating: Design, Fabrication, Ground Calibration, and 5 Years in Flight", Pub. Astron. Soc. Pacific 117, 1144-1171 (2005).
 - ⁸ B. C. Brinkman, T. Gensing, J. S. Kaastra, R. van der Meer, R. Mewe, F. B. Paerels, T. Raassen, J. van Rooijen, H. W. Braeuninger, V. Burwitz, G. D. Hartner, G. Kettenring, P. Predehl, J. J. Drake, C. O. Johnson, A. T. Kenter, R. P. Kraft, S. S. Murray, P. W. Ratzlaff, & B. J. Wargelin, "Description and performance of the low-energy transmission grating spectrometer on board Chandra", Proc. SPIE, **4012**, 81-90, 2000.
 - ⁹ *Chandra X-ray Center*, <http://chandra.harvard.edu/>
 - ¹⁰ Bavdaz, M., Wille, E., Wallace, K., Guldemann, B., Lumb, D., Martin, D., & Rando, N., "ESA optics technology preparation for IXO", SPIE 7732, 1E:1-9 (2010).
 - ¹¹ Collon, M. J., Günther, R., Ackermann, M., Partapsing, R., Vacanti, G., Beijersbergen, M. W., Bavdaz, M., Wille, E., Wallace, K., Olde Riekerink, M., Lansdorp, B., de Vreede, L., van Baren, C., Müller, P., Krumrey, M., & Freyberg, M., "Silicon-pore x-ray optics for IXO", SPIE 7732, 1F:1-9 (2010).
 - ¹² Wallace, K., Bavdaz, M., Gondoin, P., Collon, M. J., Günther, R., Ackermann, M., Beijersbergen, M. W., Olde Riekerink, M., Blom, M., Lansdorp, B., & de Vreede, L., "Silicon-pore optics development", SPIE 7437, 0T:1-9 (2009).

-
- ¹³ Collon, M. J., Guenther, R., Ackermann, M., Partapsing, R., Kelly, C., Beijersbergen, M. W., Bavdaz, M., Wallace, K., Olde Riekerink, M., Mueller, P., & Krumrey, M., "Stacking of silicon pore optics for IXO", SPIE 7437, 1A:1-7 (2009).
 - ¹⁴ Zhang, W. W., Biskach, M. P., Blake, P. N., Chan, K. W., Evans, T. C., Hong, M. L., Jones, W. D., Kolos, L. D., Mazzarella, J. M., McClelland, R. S., O'Dell, S. L., Saha, T. T., & Sharpe, M. V., "Lightweight and high angular resolution x-ray optics for astronomical missions", SPIE 8147, 0K:1-12(2011).
 - ¹⁵ Zhang, W. W., Atanassova, M., Biskach, M., Blake, P. N., Byron, G., Chan, K. W., Evans, T., Fleetwood, C., Hill, M., Hong, M., Jalota, L., Kolos, L., Mazzarella, J. M., McClelland, R., Olsen, L., Petre, R., Robinson, D., Saha, T. T., Sharpe, M., Gubarev, M. V., Jones, W. D., Kester, T., O'Dell, S. L., Caldwell, D., Davis, W., Freeman, M., Podgorski, W., Reid, P. B., & Romaine, S., "Mirror technology development for the International X-ray Observatory mission (IXO)", SPIE 7732, 1G:1-8 (2010).
 - ¹⁶ Zhang, W. W., Atanassova, M., Augustin, P., Blake, P. N., Byron, G., Carnahan, T., Chan, K. W., Fleetwood, C., He, C., Hill, M. D., Hong, M., Kolos, L., Lehan, J. P., Mazzarella, J. R., McClelland, R., Olsen, L., Petre, R., Robinson, D., Russell, R., Saha, T. T., Sharpe, M., Gubarev, M. V., Jones, W. D., O'Dell, S. L., Davis, W., Caldwell, D. R., Freeman, M., Podgorski, W. A., & Reid, P. B., "Mirror technology development for the International X-ray Observatory mission", SPIE 7437, 0Q:1-12 (2009).
 - ¹⁷ Doel, P., Atkins, C., Thompson, S., Brooks, D., Yao, J., Feldman, C., Willingale, R., Button, T., Zhang, D., & James, A., "Large thin adaptive x-ray mirrors", SPIE 6705, 0M:1-8 (2007).
 - ¹⁸ Feldman, C., Willingale, R., Atkins, C., Brooks, D., Button, T., Doel, P., James, A., Rodriguez Sanmartin, D., Smith, A., Theobald, C., Thompson, S., Wang, H., & Zhang, D., "First results from the testing of the thin shell adaptive optic prototype for high angular resolution x-ray telescopes", SPIE 7437, 1G:1-11 (2009).
 - ¹⁹ Atkins, C., Doel, P., Brooks, D., Thompson, S., Feldman, C., Willingale, R., Button, T., Rodriguez Sanmartin, D., Zhang, D., James, A., Theobald, C., Smith, A. D., & Wang, H., "Advances in active x-ray telescope technologies", SPIE 7437, 1H:1-12 (2009).
 - ²⁰ Reid, P. B., Cameron, R. A., Cohen, L., Elvis, M., Gorenstein, P., Jerius, D., Petre, R., Podgorski, W. A., Schwartz, D. A., & Zhang, W. W., "Constellation-X to Generation-X: evolution of large collecting area moderate resolution grazing incidence x-ray telescopes to larger area high-resolution adjustable optic", SPIE 5488, 325-334 (2004).
 - ²¹ Cameron, R. A., Bautz, M. W., Brissenden, R. J., Elvis, M. S., Fabbiano, G., Figueroa-Feliciano, E., Gorenstein, P., Petre, R., Reid, P. B., Schwartz, D. S., White, N. E., & Zhang, W. W., "Generation-X: mission and technology studies for an x-ray observatory vision mission", SPIE 5488, 572-580 (2004).
 - ²² Reid, P. B., Murray, S. S., Trolier-McKinstry, S., Freeman, M., Juda, M., Podgorski, W., Ramsey, B., & Schwartz, D., "Development of adjustable grazing incidence optics for Generation-X", SPIE 7011, 0V:1-10 (2008).
 - ²³ Schwartz, D. A., Brissenden, R. J., Elvis, M., Fabbiano, G., Gaetz, T. J., Jerius, D., Juda, M., Reid, P. B., Wolk, S. J., O'Dell, S. L., Kolodziejczak, J. K., & Zhang, W. W., "On-orbit adjustment calculation for the Generation-X x-ray mirror figure", SPIE 7011, 0W:1-9 (2008).
 - ²⁴ Reid, P. B., Davis, W., O'Dell, S., Schwartz, D. A., Trolier-McKinstry, S., Wilke, R. H. T., & Zhang, W., "Generation-X mirror technology development plan and the development of adjustable x-ray optics", SPIE 7437, 1F:1-10 (2009).
 - ²⁵ Schwartz, D. A., Aldcroft, T. L., Bookbinder, J. A., Cotroneo, V., Davis, W. N., Forman, W. R., Freeman, M. D., McMuldroch, S., Reid, P., Tananbaum, H., Viklinin, A., Trolier-McKinstry, S., Wilke, D., Johnson-Wilke, R., "The square-meter arcsecond-resolution x-ray telescope: SMART-X", SPIE 8503, this Volume (2012).
 - ²⁶ Feldman, C., & Willingale, R., "Piezoelectric actuation of a thin Wolter-I shell in a rigid mounting scheme", SPIE 8503, this Volume (2012).
 - ²⁷ Rodriguez Sanmartin, D., Zhang, D., Button, T., Meggs, C., Atkins, C., Doel, P., Brooks, D., Feldman, C., Willingale, R., James, A., Willis, G., & Smith, A., "Development of net-shape piezoelectric actuators for large x-ray optics", SPIE 7803, 0M:1-8 (2010).

-
- ²⁸ Atkins, C., Wang, H., Doel, P., Brooks, D., Thompson, S., Feldman, C., Willingale, R., Button, T., Rodriguez Sanmartin, D., Zhang, D., James, A., Theobald, C., Willis, G., & Smith, A. D., “Active x-ray optics for the next generation of x-ray telescopes”, SPIE 7360, 08:1-10 (2009).
- ²⁹ Atkins, C., Wang, H., Doel, P., Brooks, D., Thompson, S., Feldman, C., Willingale, R., Button, T., Rodriguez Sanmartin, D., Zhang, D., James, A., & Theobald, C., “Future high-resolution x-ray telescope technologies: prototype fabrication methods and finite element analysis”, SPIE 7011, 0X:1-12 (2008).
- ³⁰ Atkins, C., Doel, P., Brooks, D., Thompson, S., Feldman, C., Willingale, R., Button, T., Rodriguez Sanmartin, D., Zhang, D., James, A., Theobald, C., Smith, A. D., & Wang, H., “Advances in active x-ray telescope technologies”, SPIE 7437, 1H:1-12 (2009).
- ³¹ Feldman, C., Willingale, R., Atkins, C., Wang, H., Doel, P., Brooks, D., Thompson, S., Button, T., Zhang, D., Rodriguez Sanmartin, D., James, A., & Theobald, C., “Development of thin-shell adaptive optics for high angular resolution x-ray telescopes”, SPIE 7011, 0Y:1-9 (2008).
- ³² Feldman, C., Willingale, R., Atkins, C., Brooks, D., Button, T., Doel, P., James, A., Meggs, C., Rodriguez-Sanmartin, D., Smith, A., Theobald, C., & Willis, G., “The performance of thin shell adaptive optics for high angular resolution x-ray telescopes”, SPIE 7803, 0N:1-10 (2010).
- ³³ Lillie, C. F., Pearson, D. D., Cavaco, J. L., Plinta, A. D., & Wellman, J. A., “Adaptive x-ray optics development at AOA-Xinetics”, SPIE 8503, this Volume (2012).
- ³⁴ Johnson-Wilke, R. L., Wilke, R. H. T., Cotroneo, V., Davis, W. N., Reid, P. B., Schwartz, D. A., & Trolrier-McKinstry, S., “Improving yield of PZT piezoelectric devices on glass substrates”, SPIE 8503, this Volume (2012).
- ³⁵ Wilke, R. H. T., Trolrier-McKinstry, S., Reid, P. B., & Schwartz, D. A., “PZT piezoelectric films on glass for Gen-X imaging”, SPIE 7803, 0O:1-10 (2010).
- ³⁶ Cotroneo, V., Davis, W. N., Reid, P. B., Schwartz, D. A., Trolrier-McKinstry, S., & Wilke, R. H. T., “Adjustable grazing incidence x-ray optics: measurement of actuator influence functions and comparison with modeling”, SPIE 8147, 1S:1-9 (2011).
- ³⁷ Cotroneo, V., Davis, W. N., Johnson-Wilke, R.L., Marquez, V., Reid, P. B., Schwartz, D. A., Trolrier-McKinstry, S. E., & Wilke, R. H. T., “Adjustable grazing incidence x-ray optics based on thin PZT films”, SPIE 8503, this Volume (2012).
- ³⁸ Ulmer, M. P., Graham, M. E., Vaynman, S., Cao, J., & Takacs, P. Z., “Deformable mirrors for x-ray astronomy and beyond”, SPIE 8076, 05:1-10 (2011).
- ³⁹ Ulmer, M. P., Graham, M. E., Vaynman, S., Cao, J., & Takacs, P. Z., “Magnetic smart material application to adaptive x-ray optics”, SPIE 7803, 09:1-11 (2010).
- ⁴⁰ Ulmer, M. P., Wang, X., Cao, J., Savoie, J., Bellavia, B., Graham, M. E., & Vaynman, S., “Progress report on using magneto-strictive sputtered thin films to modify the shape of a x-ray telescope mirror”, SPIE 8503, this Volume (2012).
- ⁴¹ Wang, X., Cao, J., Ulmer, M. P., Graham, M. E., Vaynman, S., Savoie, J., & Bellavia, B., “Comparing theory with experimental data in studying the deformation of magnetically smart films deposited on nickel and glass substrates”, SPIE 8503, this Volume (2012).
- ⁴² Aldcroft, T. L., Schwartz, D. A., Reid, P. B., Cotroneo, V., & Davis, W. N., “Simulating correction of adjustable optics for an x-ray telescope”, SPIE 8503, this Volume (2012).

Adaptive X-ray Optics II (SPIE 8503)
2012 August 14; San Diego, CA (USA)

Toward active x-ray telescopes II

Steve O'Dell

NASA Marshall Space Flight Center
and co-authors

Co-authors represent most of community working on active x-ray telescopes.

Steve O'Dell ^a, Tom Aldcroft ^b, Carolyn Atkins ^c, Tim Button ^d, Vincenzo Cotroneo ^b, Bill Davis ^b, Peter Doel ^e, Charly Feldman ^f, Mark Freeman ^b, Mikhail Gubarev ^a, Raegan Johnson-Wilke ^g, Jeff Kolodziejczak ^a, Chuck Lillie ^h, Alan Michette ⁱ, Brian Ramsey ^a, Paul Reid ^b, Daniel Rodriguez Sanmartin ^j, Timo Saha ^k, Dan Schwartz ^b, Susan Troler-McKinstry ^g, Mel Ulmer ^l, Rudeger Wilke ^g, Dick Willingale ^f, & Will Zhang ^k

^a NASA Marshall Space Flight Center (USA)

^b Harvard-Smithsonian Center for Astrophysics (USA)

^c University of Alabama in Huntsville (USA)

^d University of Birmingham (UK)

^e University College London (UK)

^f University of Leicester (UK)

^g Pennsylvania State University (USA)

^h Lillie Consulting, with Northrop-Grumman AOA-Xinetics (USA)

ⁱ King's College London (UK)

^j University of Brighton (UK)

^k NASA Goddard Space Flight Center (USA)

^l Northwestern University (USA)

Co-authors represent most of community working on active x-ray telescopes.

Steve O'Dell ^a, Tom Aldcroft ^b, Carolyn Atkins ^c, Tim Button ^d, Vincenzo Cotroneo ^b, Bill Davis ^b, Peter Doel ^e, Charly Feldman ^f, Mark Freeman ^b, Mikhail Gubarev ^a, Raegan Johnson-Wilke ^g, Jeff Kolodziejczak ^a, Chuck Lillie ^h, Alan Michette ⁱ, Brian Ramsey ^a, Paul Reid ^b, Daniel Rodriguez Sanmartin ^j, Timo Saha ^k, Dan Schwartz ^b, Susan Trolier-McKinstry ^g, Mel Ulmer ^l, Rudeger Wilke ^g, Dick Willingale ^f, & Will Zhang ^k

^a NASA Marshall Space Flight Center (USA)

^b Harvard-Smithsonian Center for Astrophysics (USA)

^c University of Alabama in Huntsville (USA)

^d University of Birmingham (UK)

^e University College London (UK)

^f University of Leicester (UK)

^g Pennsylvania State University (USA)

^h Lillie Consulting, with Northrop-Grumman AOA-Xinetics (USA)

ⁱ King's College London (UK)

^j University of Brighton (UK)

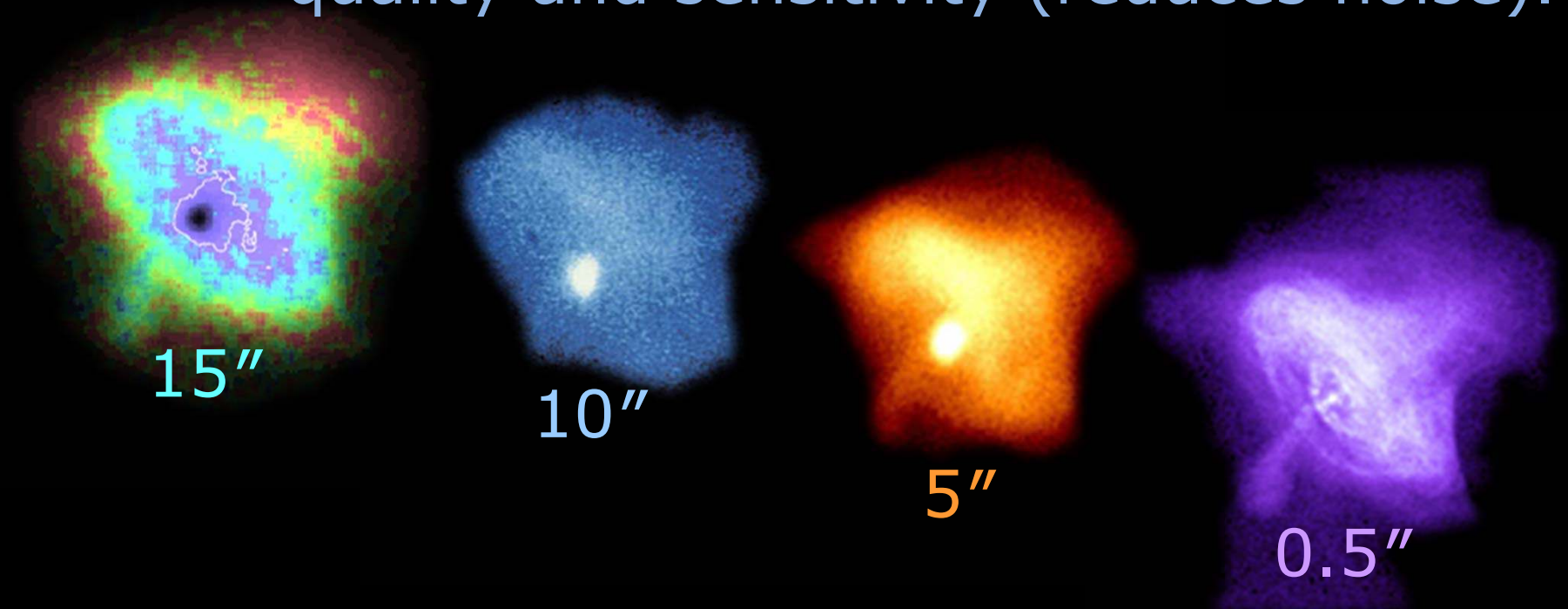
^k NASA Goddard Space Flight Center (USA)

^l Northwestern University (USA)

* presenters at this Conference

The key metrics of an x-ray telescope are angular resolution and aperture area.

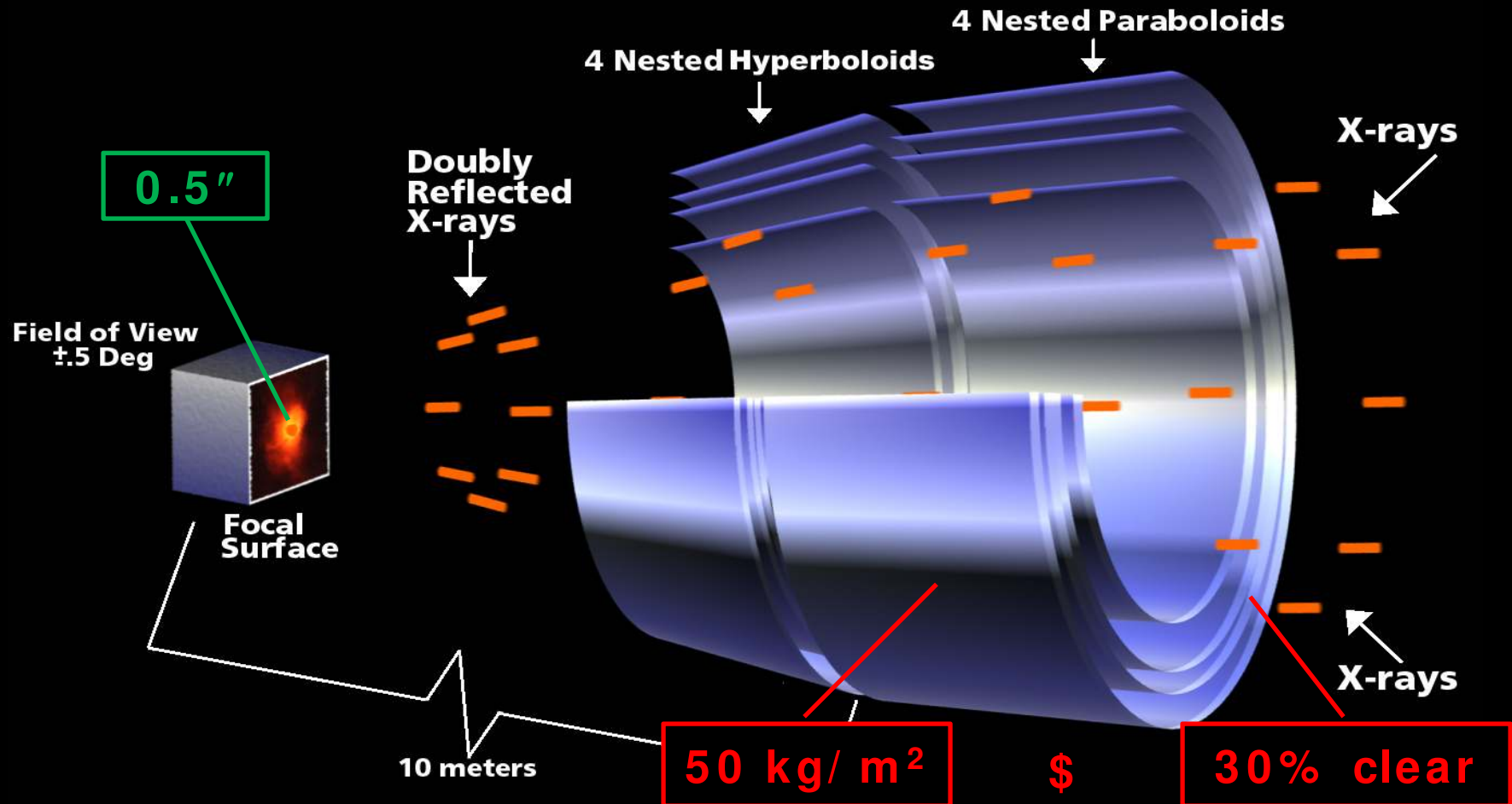
Finer angular resolution improves imaging quality and sensitivity (reduces noise).



Larger aperture area improves sensitivity (increases signal), down to the confusion limit.

Focusing x-ray telescopes utilize nested grazing-incidence (Wolter-1 like) mirrors.

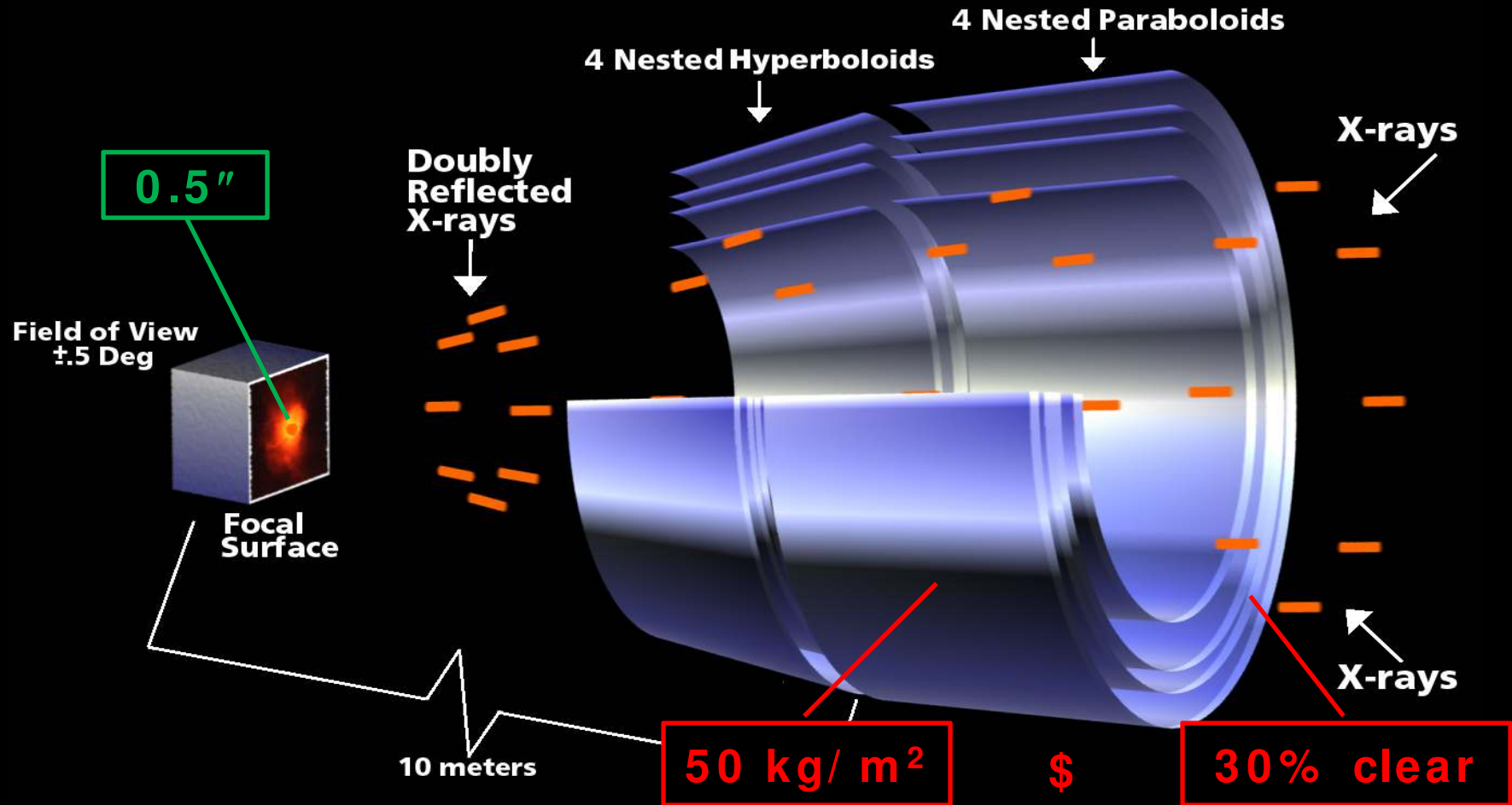
Schematic of *Chandra X-ray Observatory* x-ray telescope



Mirror elements are 0.8 m long and from 0.6 m to 1.2 m diameter

Sub-arcsec large-area x-ray telescope technologic and programmatic challenge.

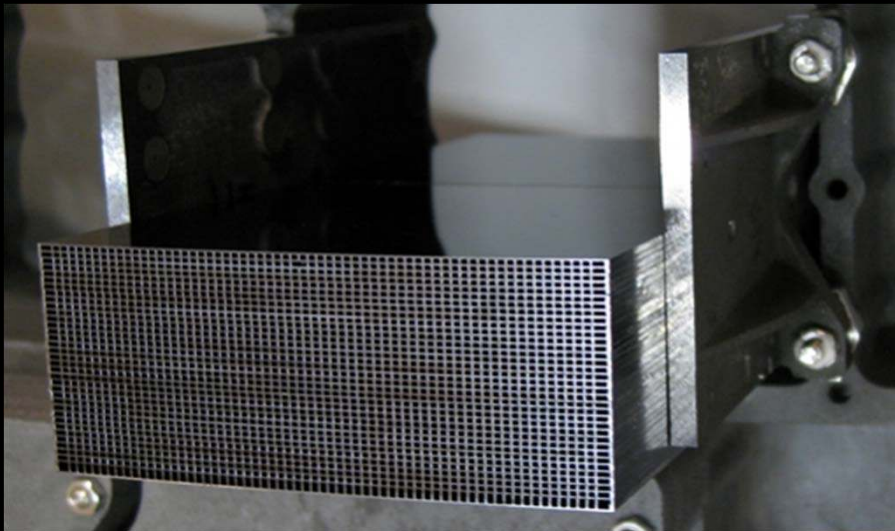
Schematic of *Chandra X-ray Observatory* x-ray telescope



Mirror elements are 0.8 m long and from 0.6 m to 1.2 m diameter

Paths to larger x-ray telescopes with $<1''$ include stiff optics and active optics.

➤ Stiff optics



- Integrated structures

➤ In any case, mirrors must be

- ❑ Lightweight and thin
- ❑ Inexpensive (e.g., replicas)
- ❑ Very good to excellent quality

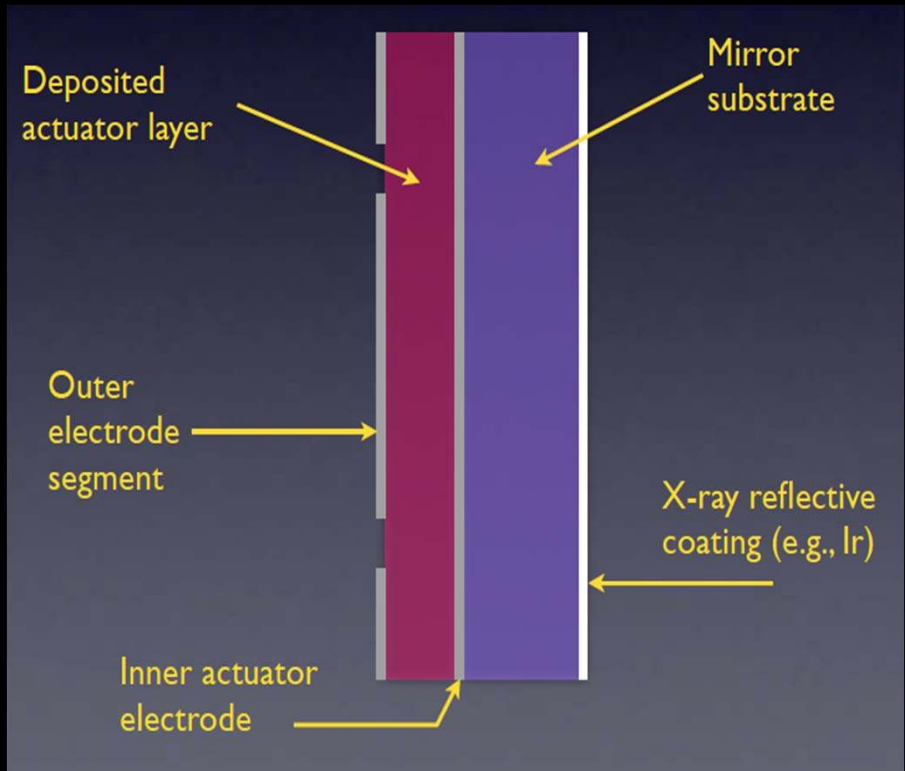
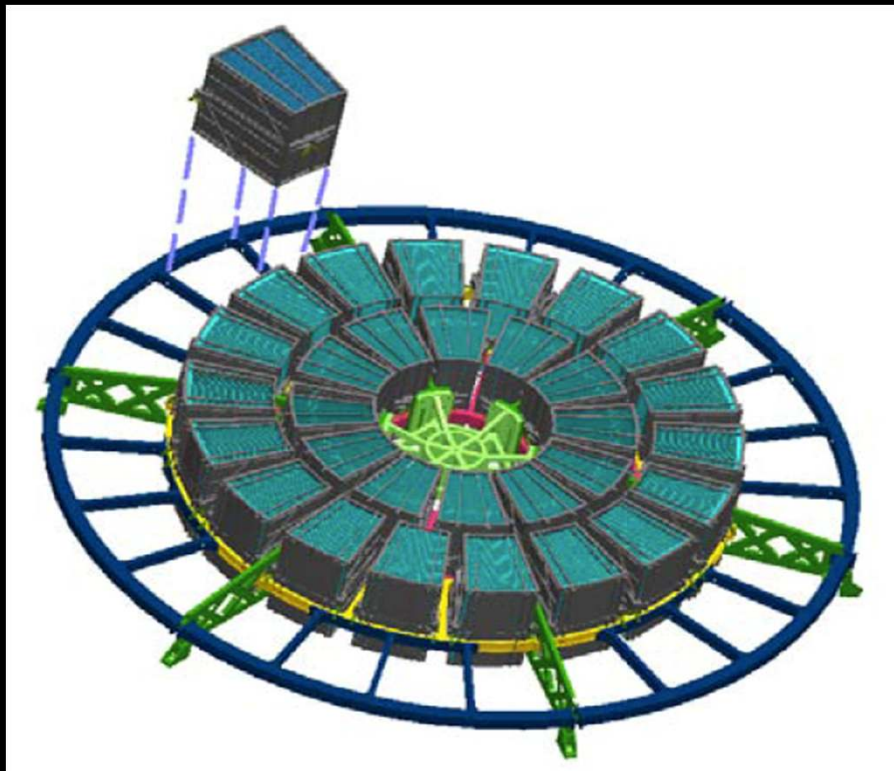
➤ Active optics

- ❑ Large normal-incidence telescopes use active optics.
 - Segment positioning
 - Curvature correction
 - Figure correction
- ❑ Large x-ray telescopes require different active-optics technologies.
 - Reaction structures for surface-normal actuation are too massive and bulky.
 - Bimorph produces surface-tangential actuation.

Approach toward a sub-arcsecond active x-ray telescope is multifaceted.

- Leverage existing x-ray technology development to start with good (HPD <5") lightweight mirrors.
 - Minimize mid- and high-frequency surface errors.
 - Minimize mount-induced distortions.
- Use surface-normal actuators to adjust alignment.
- Use surface-tangential actuator arrays to adjust low-frequency figure errors (intrinsic & mount induced).
 - Develop and test technologies for feasible STA arrays.
- Formulate strategy for on-ground and in-space image diagnostics of alignment and figure.
- Devise control algorithms and hardware for (infrequent) in-space adjustment (if needed).

SMART-X would give the sub-arcsecond resolution of *Chandra* at $\approx 30\times$ the area.

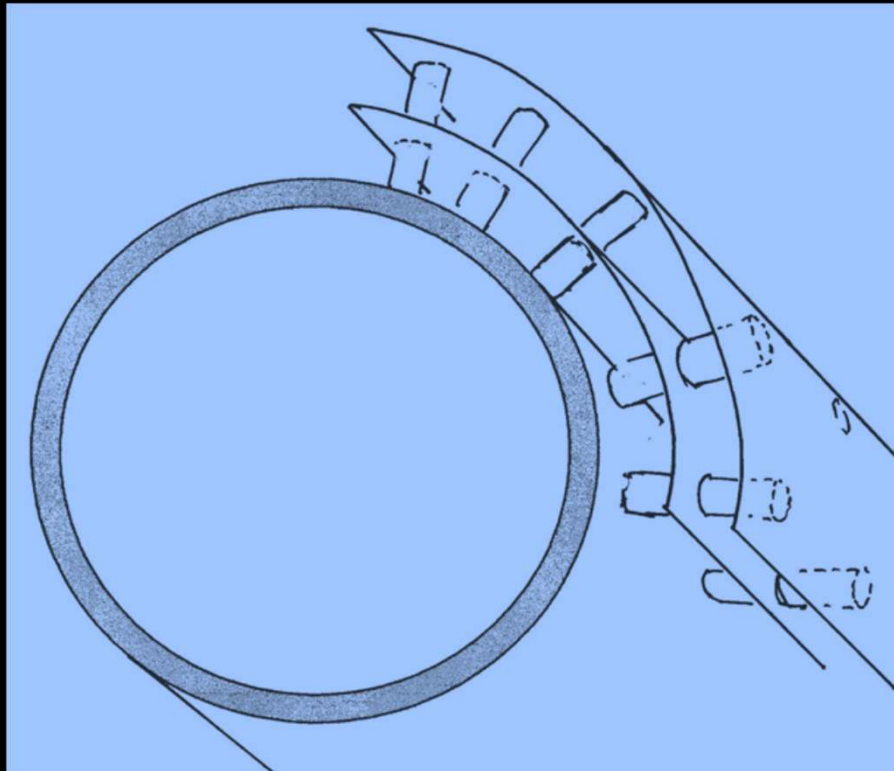


Inspired by *Chandra* experience with sub-arcsecond imaging
Leverages technology development for IXO etc. in lightweight mirrors.

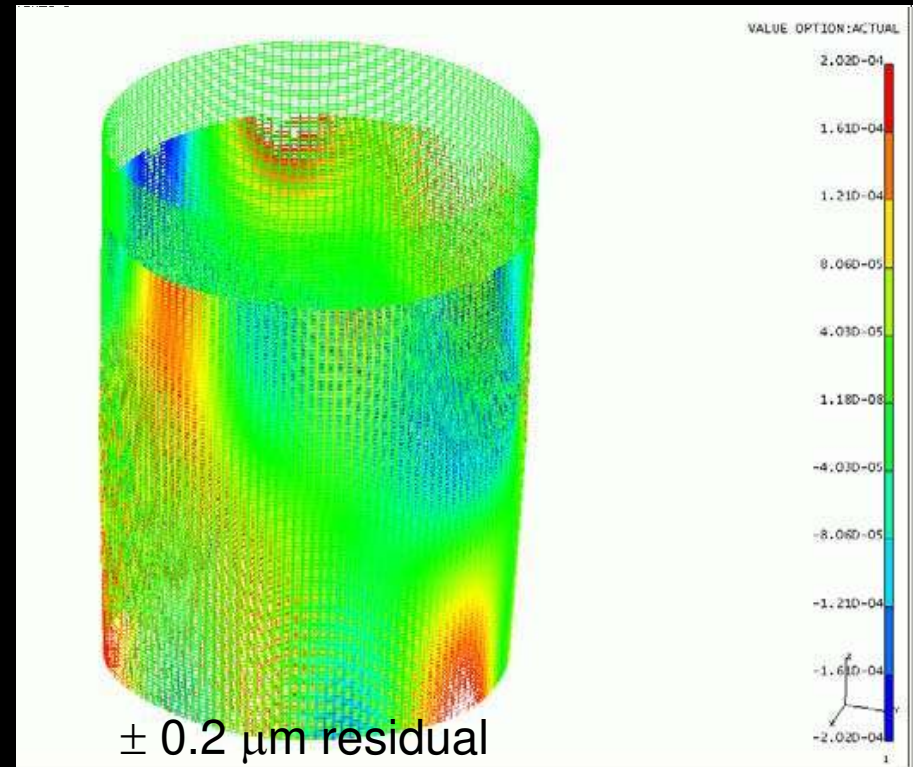
Requires initially good (5") mirrors.
Would use electro-active actuator layer to adjust figure to <1".

Dan Schwartz [8503-8]

Discrete electroactive pistons provide surface-normal actuation (SNA).



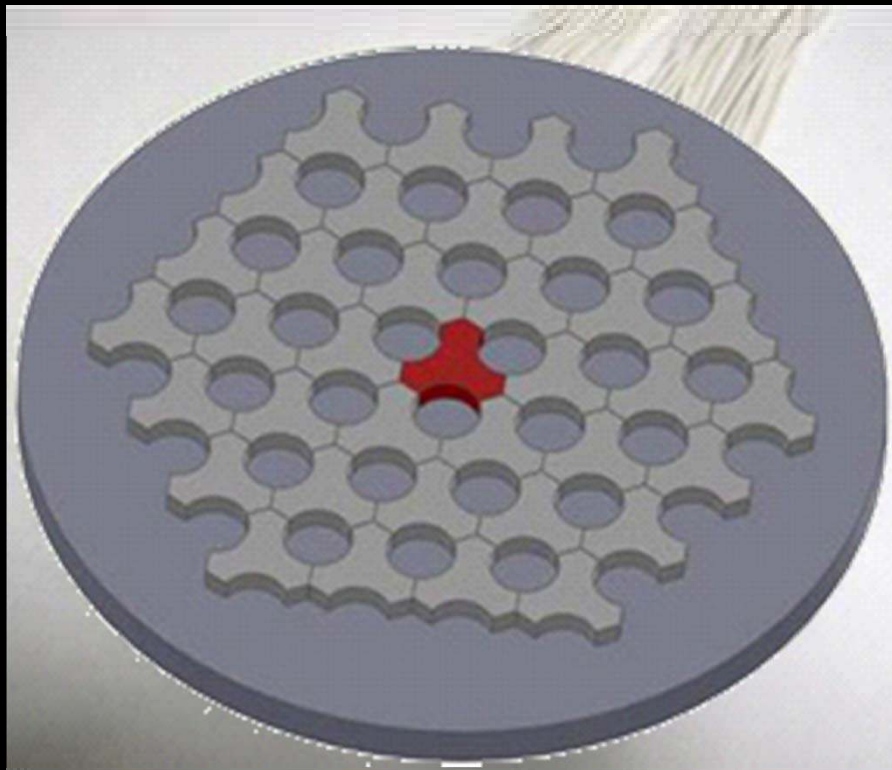
Surface normal actuation requires reaction structure.
Nested geometry limits SNA uses.
Position and steer mirror segment.



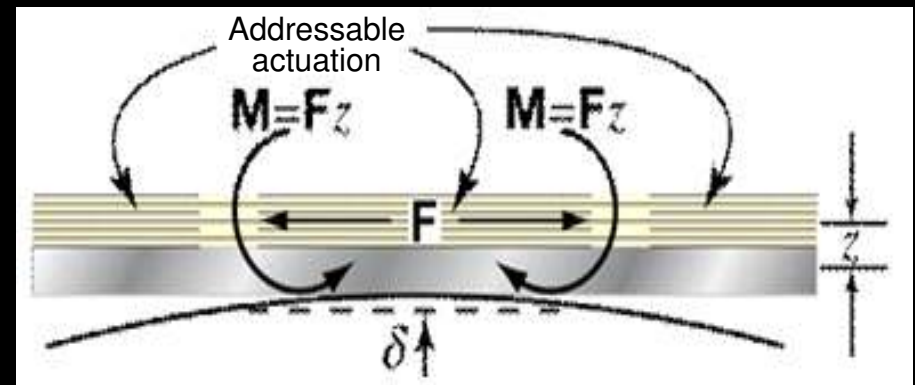
Correct large-scale distortions of full-shell mirrors.
➤ FEA uses 8×10 radial adjusters.

Paul Reid (2008)

An array of electroactive pistons provides surface-tangential actuation (STA).



An electroactive array is bonded to the back of a thin mirror. Each electrically isolated node of array is an addressable actuator.



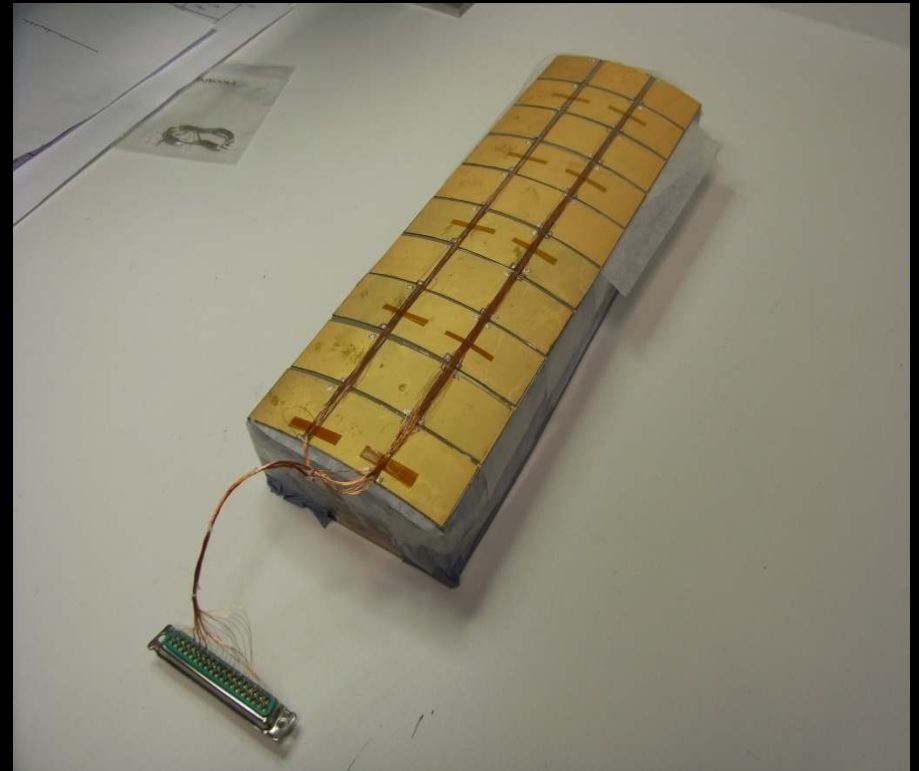
Actuation gives bimorph response. Xinetica implementation uses an electrostrictive material — PMN.

Chuck Lillie [8503-11]

Shaped piezoelectric pads, glued to back of mirror, modify the mirror's figure.



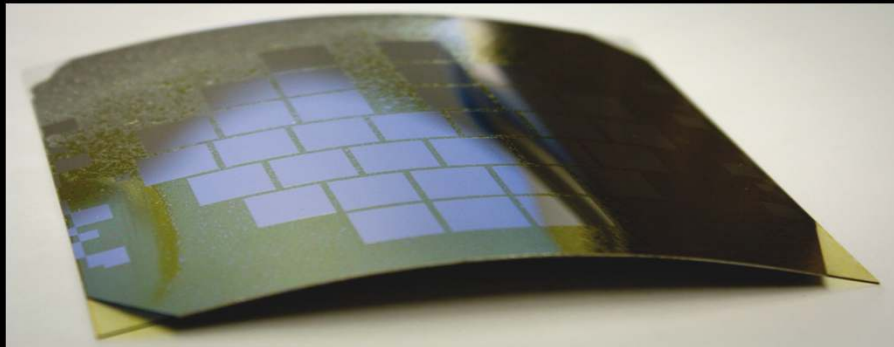
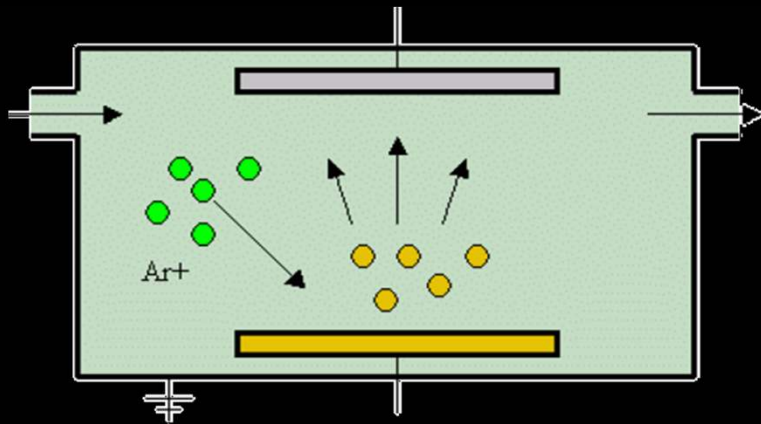
Fabrication of piezoelectric pads uses viscous plastic processing to sinter PZT formed to match the mirror's radius.



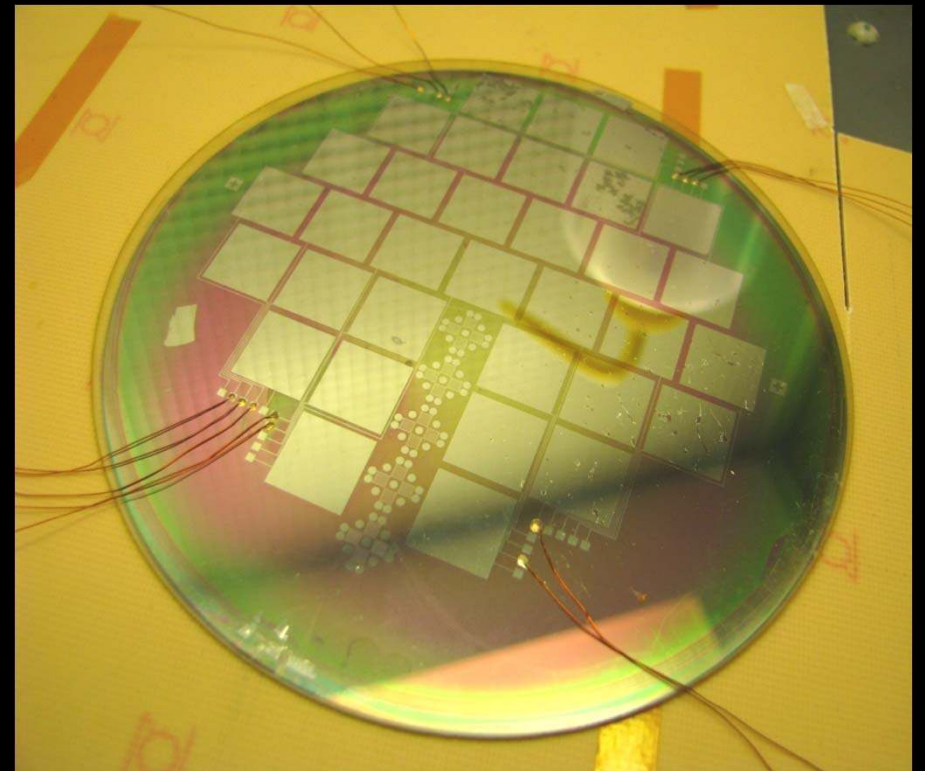
Electrical control wires lead to piezoelectric pads, glued to a 300 mm x 100 mm x 0.4 mm electroformed nickel mirror.

Charly Feldman [8503-14]

An electroactive thin film with patterned electrodes provides (bimorph) STA array.



Use slumped-glass substrate.
Deposit piezoelectric (PZT) on back; crystallize, anneal at high T.
Deposit electrode array and traces.



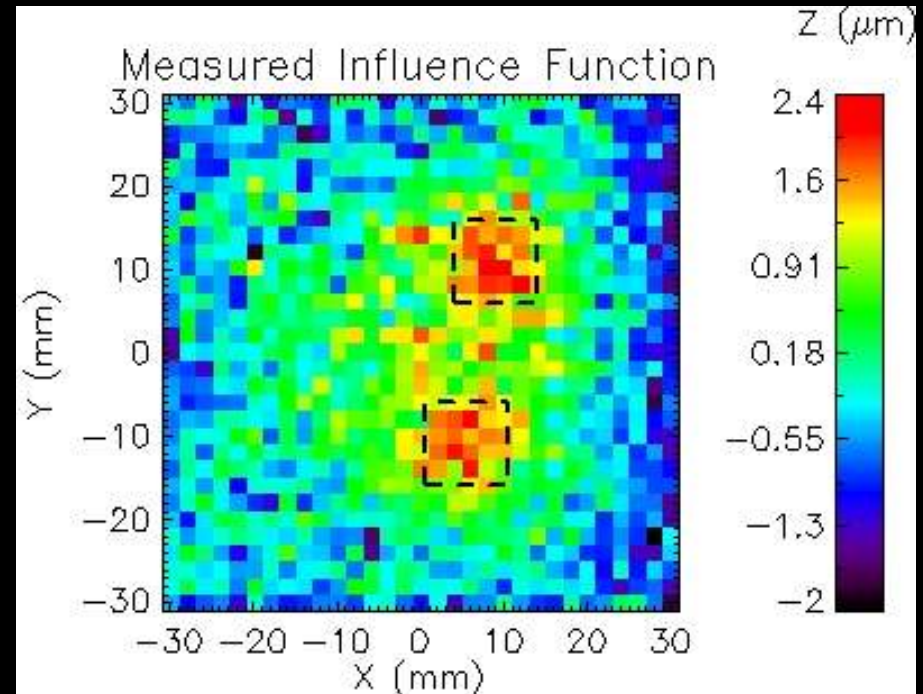
Produced flat coupons for process development and to measure the influence function.

Raegan Johnson-Wilke [8503-10]

Measurement of influence function shows semi-quantitative agreement with FEA.

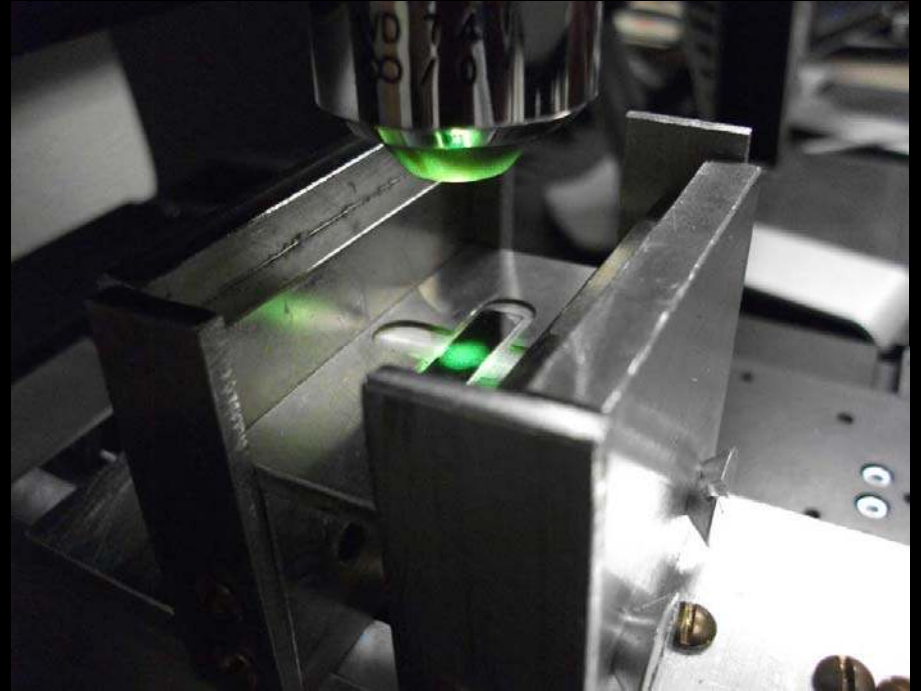


Attach mirror with thin-film STA array on back, into holder.
Perform metrology of active mirror in null and various actuated states.



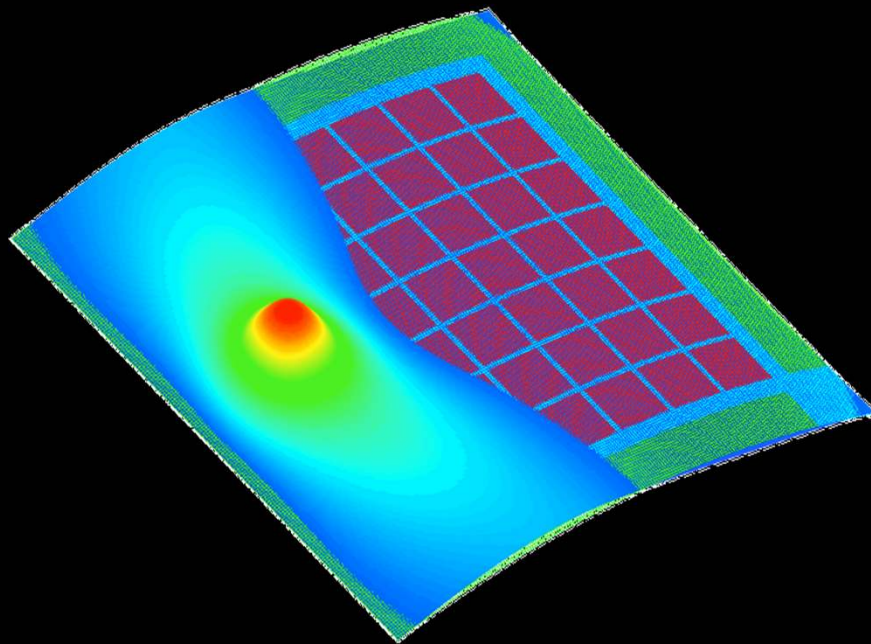
Compare measured influence function with FEA prediction.

Vincenzo Cotroneo [8503-9]

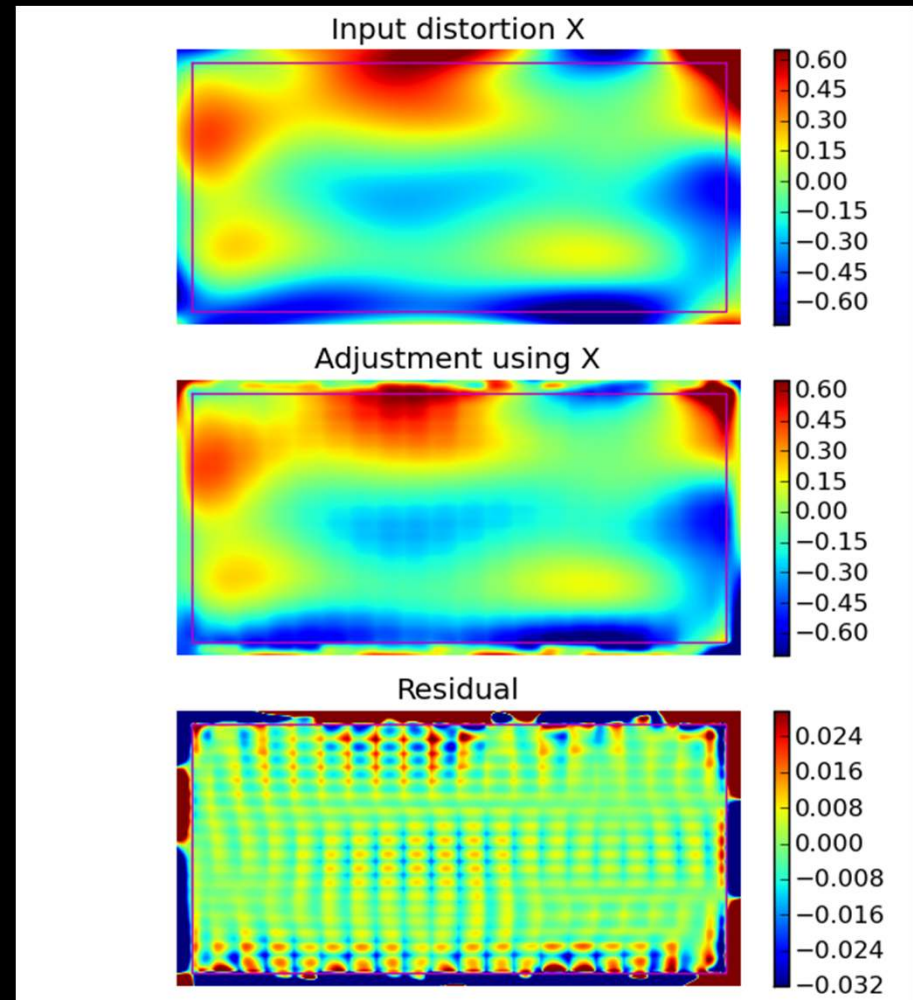


Mel Ulmer[8503-12]
Xiaoli Wang [8503-13]

Simulate figure correction using influence function measured



FEA computes influence function for each actuator



Tom Aldcroft [8503-15]

Co-authors for Toward Active X-ray Telescopes II

Presented by Steve O'Dell

Steve O'Dell a, Tom Aldcroft b, Carolyn Atkins c, Tim Button d, Vincenzo Cotroneo b, Bill Davis b, Peter Doel e, Charly Feldman f, Mark Freeman b, Mikhail Gubarev a, Raegan Johnson-Wilke g, Jeff Kolodziejczak a, Chuck Lillie h, Alan Michette i, Brian Ramsey a, Paul Reid b, Daniel Rodriguez Sanmartin j, Timo Saha k, Dan Schwartz b, Susan Trolier-McKinstry g, Mel Ulmer l, Rudeger Wilke g, Dick Willingale f, & Will Zhang k

a NASA Marshall Space Flight Center (USA)

b Harvard-Smithsonian Center for Astrophysics (USA)

c University of Alabama in Huntsville (USA)

d University of Birmingham (UK)

e University College London (UK)

f University of Leicester (UK)

g Pennsylvania State University (USA)

h Lillie Consulting, with Northrop-Grumman AOA-Xinetics (USA)

i King's College London (UK)

j University of Brighton (UK)

k NASA Goddard Space Flight Center (USA)

l Northwestern University (USA)